From THE DEPARTMENT OF PHYSIOLOGY AND PHARMACOLOGY
Karolinska Institutet, Stockholm, Sweden

THE CIRCUIT AND SYNAPTIC ORGANIZATION OF THE BASAL GANGLIA OUTPUT: MECHANISTIC INSIGHTS ON MOVEMENT DISORDERS AND ACTION CONTROL

Giacomo Sitzia

Stockholm 2022

Published by Karolinska Institutet.
Printed by Universitetsservice US-AB, 2022

ISBN 978-91-8016-820-5
Cover illustration: *A collage on canvas of neurons and receptors by Matisse; Generated by Giacomo Sitzia using DALL·E*.

The circuit and synaptic organization of the basal ganglia output: mechanistic insights on movement disorders and action control

By

Giacomo Sitzia

The thesis will be defended in public at the Rockefeller lecture hall, Karolinska Institutet, November 8, 2022, at 9:00 am

Principal Supervisor:
Karima Chergui
Karolinska Institutet
Department of Physiology and Pharmacology

Co-supervisor(s):
David M. Lovinger
National Institutes on Alcoholism and Alcohol Abuse
Laboratory for Integrative Neuroscience

Xiaoqun Zhang
Karolinska Institutet
Department of Clinical Neuroscience

Per Svenningsson
Karolinska Institutet
Department of Clinical Neuroscience

Opponent:
Alexandra Nelson
University of California San Francisco
Department of Neurology

Examination Board:
Gilad Silberberg
Karolinska Institutet
Department of Neuroscience

Louise Adermark
University of Gothenburg
Department of Pharmacology

Åsa Mackenzie
University of Uppsala
Department of Organismal Biology

A Giorgia, Babbo, Mamma, Luca

POPULAR SCIENCE SUMMARY OF THE THESIS

Parkinson's disease is a movement disorder affecting an increasingly high number of people worldwide. Alcohol use disorder has devastating consequences on individual's health and on society. At a first sight, these two conditions might seem unrelated. But neuroscience has realized that they are not. This thesis examined what's in common between these two diseases: brain circuits.

Nervous systems across all mammals and even very ancient vertebrates maintain a common organizational backbone that allows them to adapt to an ever-changing environment. This includes the ability to decide if and how to move, for what motivation, and to learn to control movements. Let's say you want to make a purposeful action and keep reading this thesis. This will engage the basal ganglia, a part of the brain at the intersection between cognition and movement.

This thesis focused on neurons, the brain cells that receive and transmit signals through synaptic communication. One type of synaptic communication is chemical and involves a neuron that sends an input via releasing a small molecule, and a neuron that senses and reacts to that small molecule through dedicated proteins. In disease, brain circuits and the resulting behavioral outputs are changed because of the death of a group of neurons, a change in the organization of the synapses, and very often a combination of the two.

One part of my thesis was dedicated to understanding how basal ganglia circuits are rearranged by modeling Parkinson's Disease in mice. The mouse basal ganglia have a similar circuitry to those of humans. Parkinson's Disease is caused by the death of crucial cells that release the neuromodulator dopamine, a master regulator of basal ganglia circuit function. By chemically inducing dopaminergic cell death in mice, we were able to ask the question: what happens to chemical synapses in the basal ganglia when dopamine is not there anymore? A second part of my thesis analyzed brain circuits dedicated to purposeful or automated action control were arranged and modified by chronic alcohol exposure.

A lot remains to be learned about how synapses in the basal ganglia are organized and how this contributes to generate simple and complex movements.

ABSTRACT

Understanding the neural circuitry underlying movement is a neuroscientific challenge that promises to help refining currently available treatments for movement disorders. Key structures for movement and action control are the basal ganglia nuclei, whose complexity has only just started to be resolved. The constituent papers of this thesis analyzed different levels of basal ganglia circuit organization and function.

In **paper 1** we used a 6-hydroxydopamine (6-OHDA) lesion model of Parkinson's Disease (PD) to study glutamatergic synapses in the substantia nigra reticulata (SNr). We found that NMDA receptors synaptic function in the SNr is altered in 6-OHDA lesioned mice. NMDA receptor blockade transiently rescued hypolocomotion in 6-OHDA lesioned mice. In **paper 2** we used a mutated Leucin Rich Repeat Kinase 2 (LRRK2-G2019S) mouse model and studied midbrain adaptations in a middle age range that precedes the onset of neurodegeneration. LRRK2-G2019S mice had increased exploratory behavior compared to their wild-type littermate. In midbrain dopamine neurons glutamatergic neurotransmission was affected in a region-specific manner, but no change in firing was identified. In **paper 3** we used the same model to investigate the firing and glutamatergic synapses of SNr neurons. We found no change in firing whereas glutamate release but not N-Methyl-D-Aspartate (NMDA) receptors was altered in SNr neurons. In **paper 4** we analyzed the organization of synaptic inputs to the associative and sensorimotor SNr. We found that inputs from the direct pathway are homogeneously distributed across SNr subregions whereas inputs from the indirect pathway are biased to the sensorimotor SNr. In alcohol exposed mice, inputs from the sensorimotor striatum were selectively potentiated. In **paper 5** we focused on the indirect pathway projections to the globus pallidus external segment and identified distinct mechanisms of presynaptic modulation by cannabinoid 1 (CB1) and $GABA_B$ receptors.

In summary, we have investigated several basal ganglia circuits and their synaptic adaptations in disease models. We revealed key features of the SNr circuit organization and its adaptations in mouse models of PD. We found that distinct subpopulations of SNr neurons are part of the associative and sensorimotor loops, and that direct and direct pathway inputs are differentially integrated in these neurons. These findings are relevant to understanding how the SNr shapes the behavioral output of the basal ganglia circuits. In mouse models of PD and alcohol use disorder the synaptic inputs to the SNr are reorganized. These findings open novel views and research directions on the functional organization of the basal ganglia output.

LIST OF SCIENTIFIC PAPERS

I. NMDA receptors are altered in the substantia nigra reticulata and their blockade ameliorates motor deficits in experimental parkinsonism
***Sitzia G.**, Mantas I., Zhang X., Svenningsson P., Chergui K., Neuropharmacology, 2020*

II. LRRK2-G2019S mice display alterations in glutamatergic synaptic transmission in midbrain dopamine neurons
*Skiteva O., Yao N., **Sitzia G.**, Chergui K. Journal of neurochemistry, 2022*

III. Neuronal firing and glutamatergic synapses in the substantia nigra pars reticulata of LRRK2-G2019S mice
***Sitzia G.**, Skiteva O., Chergui K.. Manuscript, 2022*

IV. Input-specific plasticity on distinct basal ganglia output subdomains underlies action performance deficits following chronic ethanol exposure
***Sitzia G.**, Bariselli S., Gracias A., Lovinger DM. Manuscript, 2022*

V. Distinct mechanisms of CB1 and GABAB receptor presynaptic modulation of striatal indirect pathway projections to mouse Globus Pallidus
***Sitzia G.,** Abrahao KP., Liput D., Calandra GM., Lovinger DM. Manuscript, 2022*

CONTENTS

LIST OF ABBREVIATIONS

AUD	Alcohol Use Disorder
BG	Basal Ganglia
BLA	Basolateral Amygdala
CeA	Central Amygdala
DBS	Deep Brain Stimulation
DLS	Dorsolateral striatum
DMS	Dorsomedial Striatum
dSPNs	Direct pathway SPNs
FoxP2	Forkhead box P2
GAD2	Glutamate Decarboxylase 2
GPCRs	G-Protein-Coupled-Receptors
GPe	Globus Pallidus External segment
GPi	Globus Pallidus Internal segment
iSPNs	Indirect pathway SPNs
L-DOPA	l-3,4-dihydroxyphenylalanine
LH	Lateral Habenula
LHX6	LIM Homeobox 6
LRRK2	Leucine Rich Repeat Kinase 2
MLR	Mesencephalic Locomotor Region
NAc	Nucleus Accumbens
Nkx2.1	NK2 homeobox 1
NMDAR	N-Methyl-D-Aspartate receptor
Npas1	Neuronal PAS Domain Protein 1
PD	Parkinson’s Disease
Pf	Parafascicular Thalamus
PV	Parvalbumin

RBP4	Retinol Binding Protein 4
SNc	Substantia Nigra pars Compacta
SNr	Substantia Nigra Reticulata
SPNs	Spiny Projection Neurons
SST	Somatostatin
STN	Subthalamic Nucleus
TRN	Thalamic Reticular Nucleus
VGluT2	Vesicular Glutamate Transporter 2
VP	Ventral Pallidum
VTA	Ventral Tegmental Area
WHO	World Health Organization

1 INTRODUCTION

The ability to move and produce purposeful or automated actions is paramount for adaptive behavior. The basal ganglia (BG) are brain structures critical for action and movement control whose function is compromised in Parkinson's Disease (PD), a movement disorder characterized by severe motor and non- motor symptoms. Other diseases including Alcohol Use Disorder (AUD) affect the functioning of the BG. PD patients experience difficulties in moving and performing actions that are essential for their daily lives, whereas the life of persons with AUD is perturbed by uncontrolled drinking. Neuroscience aims at understanding how brain circuits are organized and impacted by disease, with the highest goal of producing knowledge that will ultimately help in making a positive impact in the lives of those who suffer.

This thesis tackles scientific questions that regard the circuit organization of the BG output structure, the Substantia Nigra pars Reticulata (SNr), and its dysfunctions in PD and AUD. It also considers aspects of the physiology and pharmacology of key G-Protein-Coupled-Receptors (GPCRs) in the Globus Pallidus external segment (GPe) and N-Methyl-D-Aspartate (NMDA) receptors in the SNr.

2 ORGANIZATION OF BASAL GANGLIA CIRCUITS

The BG are a group of anatomically distinct nuclei located in the forebrain and midbrain. Their nomenclature originates from early anatomical studies that for the first time identified them and described them as separate 'ganglia' (term nowadays replaced by nuclei) located at the base of the brain, hence 'basal' (Ferrier, 1876). A commonly used formula in modern literature refers to the BG nuclei as s*trictly interconnected* structures. The BG are embedded on a larger network including cortical, thalamic, midbrain and brainstem nuclei. This interconnectivity came to be fully appreciated thanks to the refinement of anatomical tracing methods pinnacling in the 1960s (Haber et al., 2016; Nauta & Mehler, 1966). 60 years later, the anatomical and cellular organization of the BG continues to be refined, and much remains to be discovered about their function.

2.1 THE BASAL GANGLIA NUCLEI AND THEIR INTERCONNECTIONS

The Striatum

The term 'striatum' identifies the largest structure of the BG. In the human brain the striatum is a continuous mass consisting of two subdivisions, the putamen and caudate nuclei, which are divided by the internal capsule, a dense bundle formed by corticofugal and corticopetal fibers. The rostroventral subdivision of the striatum is referred to as ventral striatum, or nucleus

accumbens (Nac). In rodents, the striatum forms a continuous mass and lacks an anatomical landmark to separate its putamen-equivalent subdivision, the Dorsal Lateral Striatum (DLS), from its caudate-equivalent subdivision, the Dorsal Medial Striatum (DMS). In rodents the NAc constitutes the rostral, ventromedial portion of the striatum.

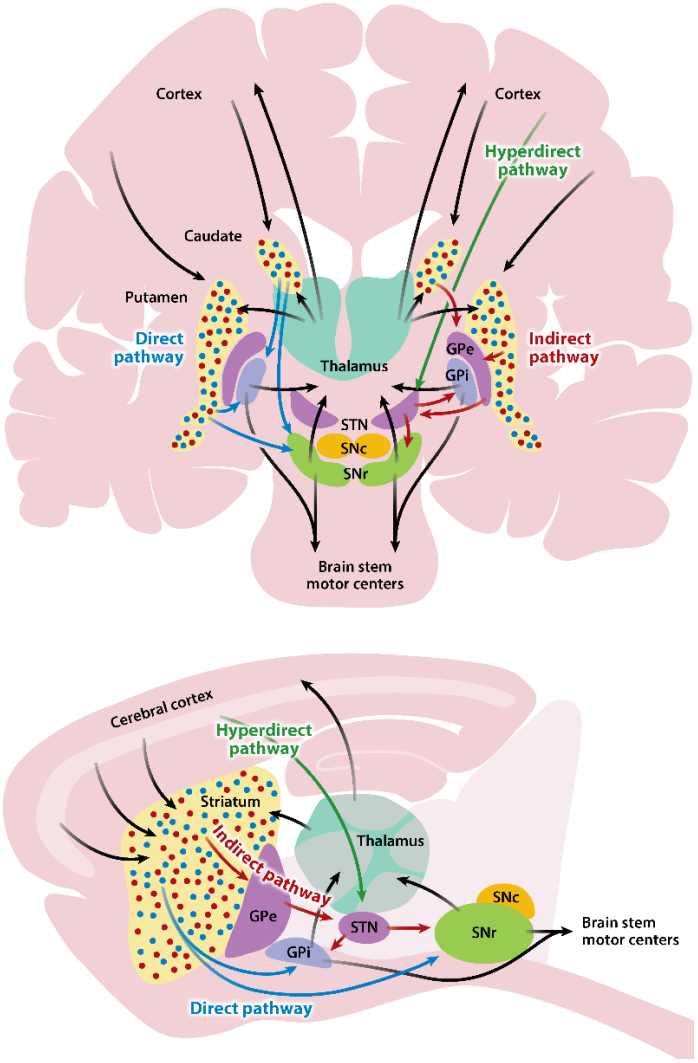

Figure 1 Main projections of the BG circuitry in the Human (Top) and rodent (Bottom) brain. Reprinted with permission from Nelson & Kreitzer, 2014

Extrinsic inputs are integrated in the dorsal striatal microcircuitry that consists of locally-projecting GABAergic and cholinergic interneurons (in total ~5% of the total neurons) and of downstream projecting but also locally branching Spiny Projection Neurons (SPNs) (Fig 1) (in total ~95% of striatal neurons) (Burke et al., 2017; Gerfen et al., 1990; Silberberg & Bolam, 2015). The striatal SPNs are the long-range projecting GABAergic neurons and are divided into direct pathway SPNs (dSPNs) and indirect pathway SPNs (iSPNs) on the basis of their molecular identity and projection targets (Alexander et al., 1986; Gerfen et al., 1990). dSPNs express the dopamine D1 receptor and project to the Globus Pallidus internal segment (GPi) and SNr to form the direct pathway, while also collateralizing to the GPe to form the ’bridge

collateral' projection (Chang et al., 1980; Cui et al., 2021; Lévesque & Parent, 2005). iSPNs express the dopamine D2 receptor and project exclusively to the GPe (Alexander et al., 1986; Gerfen et al., 1990). The striatum contains the most neurons and receives the largest number of extrinsic inputs among all basal ganglia nuclei. These include excitatory inputs from nearly every cortical area as well as thalamic and amygdalar inputs, as well as neuromodulatory inputs including the prominent dopaminergic input from the substantia nigra pars compacta (SNc) . Overall, the striatum is well poised to integrate high-order cortical and thalamic inputs with state- related neuromodulatory inputs to inform its downstream targets (Dudman & Krakauer, 2016; Redgrave et al., 2010).

A reference model of BG circuit organization: *The classical model incorporated anatomical, physiological and clinical evidence to propose a functional organization of the BG. In the model, the direct pahtway originates from striatal dSPNs targeting the GPi/ SNr to inhibit their tonic firing activity, thus disinhibiting their thalamic and brainstem targets to produce a net excitatory effect on the cortical and behavioral output. The indirect pahtway originates from striatal iSPNs which inhibit their tonically active GPe targets. This results in a disinhibition of the subthalamic nucleus that via excitatory inputs to the GPi/ SNr inhibits the cortical and behavioral outputs. Striatal dopamine exerts a net excitatory effect on the direct pathway via the activation of the $G_{\alpha olf}$-coupled D1-like receptors on dSPNs and a net inhibitory effect on the indirect pathway via the activation of G_I- coupled D2- like receptors on iSPNs (Albin et al., 1989; Alexander & Crutcher, 1990; DeLong, 1990; Tritsch and Sabatini, 2012).*

The Globus Pallidus External Segment

The GPe is located caudomedially from the striatum by which it is distinguished by its pale appearance given by the presence of striatofugal myelinated fibers, hence the latin denomination 'pallidus'. The GPe is constituted by GABAergic neurons projecting to downstream and upstream BG and extra-BG targets while also collateralizing locally. Subpopulations of acetylcholine releasing neurons have also been identified. The primary GABAergic input arises from striatal iSPNs part of the indirect pathway. Additional GABAergic inputs include the striatal dSPN bridge collaterals, GPi inputs and local collaterals primarily from *Parvalbumin* (PV) expressing neurons (Gittis et al., 2014; Higgs et al., 2021). The GPe integrates glutamatergic inputs from the STN and extra-BG regions including central amygdala (Giovanniello et al., 2020), cortex (Abecassis et al., 2020) and thalamus (Naito & Kita, 1994; Yasukawa et al., 2004). There is large consensus about the presence of two main subtypes of GPe neurons. Arkypallidal GPe neurons constitute ~30 % of GPe neurons. They

are pacemaking, project to the striatum and express distinctive markers including *Forkhead box P2* (FoxP2) and *Neuronal PAS Domain Protein 1* (Npas1) (Abdi et al., 2015; Hernández et al., 2015; Mallet et al., 2012). The signal provided by arkypallidal GPe neurons to the striatum has an inhibitory effect on movement and action performance (Aristieta et al, 2021; Mallet et al., 2016). Two recent studies converged in indicating dSPNs bridge collaterals as the primary source of striatal innervation of arkypallidal GPe neurons (Cui et al., 2021; Ketzef & Silberberg, 2021). A subpopulation of *LIM Homeobox 6 (*Lhx6) neurons co-expressing Nkx2.1/Npas1 neurons has been reported to project to the cortex, midbrain and Thalamic Reticular Nucleus (TRN) (Abecassis et al., 2021). The largest subtype of GPe neurons, constituting ~50% of the total population, are 'prototypic' neurons that fire at high, regular frequencies, project to intra-BG targets including the STN, GPi and SNr and have been first characterized for the co-expression of Nkx2.1 and Lhx6 (Abdi et al., 2015; Hernández et al., 2015; Mallet et al., 2012; Mastro et al., 2014). The majority of prototypic GPe neurons co-express Lhx6/Nkx2.1/PV (Abdi et al., 2015), however a subtype of Pf thalamus projecting PV^+ neurons does not co-express Lhx6 (Lilascharoen et al., 2021; Saunders et al., 2015). $Lhx6^+$ GPe neurons preferentially innervate the SNc over the SNr, whereas PV^+ GPe neurons preferentially innervate the SNr (Evans et al., 2020; Mastro et al., 2014). A third subtype of GPe neurons projecting to the frontal cortex and co-releasing GABA and acetylcholine has been characterized for the co-expression of the Choline Acetyl Transferase (ChAT) and Nkx2.1 (Abdi et al., 2015; Saunders et al., 2015). In contrast with the arkypallidal subpopulation of GPe neurons, prototypic GPe neurons have been found to be the primary target of the striatal iSPNs indicating that they are embedded in the indirect pathway (Cui et al., 2021; Ketzef & Silberberg, 2021). Taken together, the GPe is a highly heterogeneous region that is both intrinsic to the BG but also possesses extra-BG inputs and outputs.

The Subthalamic Nucleus

The Subthalamic Nucleus (STN) is a lenticular nucleus located ventrally from the thalamus, constituted by densely packed GLUergic neurons. Coherently with their GLUergic identity the majority of STN neurons are characterized by the expression of the Vesicular Glutamate Transporter (VGluT2) (Schweizer et al., 2015). A recent study identified spatially segregated patterns of gene expression in the STN indicating the presence of molecularly different subpopulations of STN neurons, including a subpopulation of molecularly identified GABAergic neurons (Wallén-Mackenzie et al., 2020). In addition to their BG targets, i.e., the GPe and SNr, STN neurons have also been shown to project to the Ventral Pallidum (VP), a brain region associated with valence (Fife et al., 2017; Ketzef & Silberberg, 2021; Stephenson-

Jones et al., 2016; Pamucku et al., 2020; Serra et al., 2020; Tooley et al., 2018). Additional STN projection targets include the zona incerta (ZI) and several brainstem nuclei (Kita & Kita, 2012). The STN receives a prominent GABAergic innervation from prototypic GPe neurons (Abdi et al., 2015; Hernández et al., 2015; Mallet et al., 2012). A prominent input to the STN is represented by the cortical 'hyperdirect' projection (Afsharpour, 1985; Kita et al., 2014) which was excluded by initial circuit maps of the BG. An additional STN input originates in the parafascicular (Pf) thalamus (Féger et al., 1994; Watson et al., 2021). Overall, the STN integrates complex intra-BG and extra-BG inputs to provide the primary source of innervation of the BG output structures, the GPe and additional forebrain and midbrain targets.

The BG outputs

The BG output is constituted by two nuclei, the GPi and SNr. The relative contribution of the GPi and SNr as BG outputs is different across species, in that the GPi is the main output in humans and other primates and the SNr the main output in rodents. The organization of the SNr will be discussed in detail later in this introduction. The GPi is often referred to as 'entopeduncular nucleus' in rodents. The remainder description will consider the GPi connectivity in rodents. The GPi is innervated by dSPNs and ^{PV}GPe GABAergic and STN GLUergic inputs (Miyamoto & Fukuda, 2022; Rajakumar et al., 1994; Weglage et al., 2022; Van Der Kooy & Carter, 1981). GPi neurons are distinct in two subpopulations of GABAergic, PV^+ neurons projecting to thalamic and brainstem regions, and Somatostatin (SST) expressing neurons projecting to the Lateral Habenula (LH) and co-releasing GABA and GLU (Shabel et al., 2014; Weglage et al., 2022). Additional targets of GPi SST^+ neurons include the GPe, striatal striosomes and the SNc (Weglage et al., 2022). Hence, the GPi functions as a BG output but also signals as a feedback structure to other nuclei of the BG.

2.2 PARALLEL CIRCUIT ORGANIZATION

The BG are involved in numerous functions ranging from motor control to executive functions to the control of emotions. In addition to the direct/ indirect pathway divide, functional differentiation in the BG circuitry has also been postulated based on the patch/ matrix divide and on the medio-lateral divide (Gerfen et al., 1992). The patch/ matrix hypothesis is based on the existence of molecularly identified striatal striosome (patch) subcompartments constituting up to 15% of the striatal volume and identified based on the enrichment of MORs, reduced expression of calbindin and specific input/ output connectivity (Kuhar et al., 1973; Gerfen et al., 1992; McGregor et al., 2019; Ragsdale & Graybiel, 1988; Xiao et al., 2020). Striosomal and matrix neurons project to the dSPN canonical target SNr but in addition striosomal neurons

also project to the SNc (Gerfen, 1992; McGregor et al., 2019; Xiao et al., 2020). Striosomal neurons are preferentially innervated by limbic cortical inputs and amygdalar inputs compared to matrix neurons (Crittenden & Graybiel, 2011; McGregor et al., 2019; Ragsdale & Graybiel, 1988). In the remainder of this paragraph the medio-lateral divide will be considered in greater detail with a special focus on the corticostriatal projections.

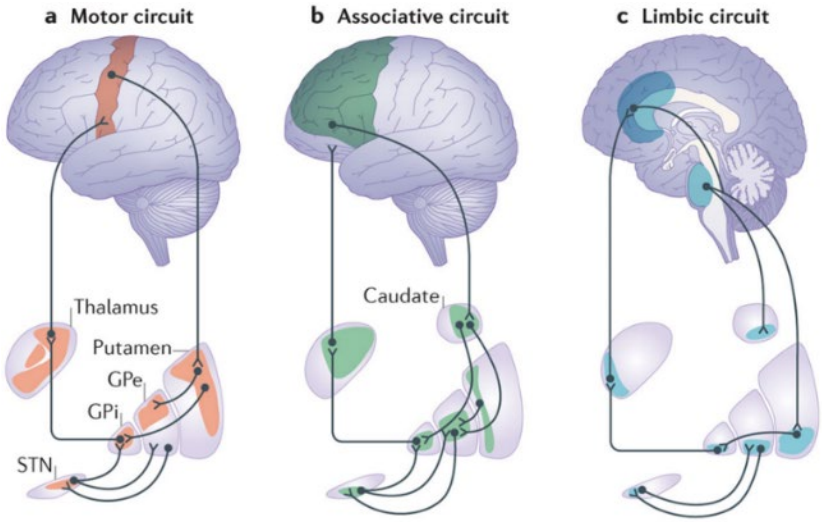

Figure 2: Parallel circuit organization of the basal ganglia. Reprinted with permission from (Jahanshahi et al., 2015).

Cortico-striatal projections are organized in a topographic fashion delimitating distinct functional territories in the striatum (Hintiryan et al., 2016; Hunnicutt et al., 2016; Gerfen et al., 1992). A similar topographic organization is maintained on striatal efferent projections to the GPe and further preserved throughout the entirety of cortico-BG-thalamo-cortical loops (Lee et al., 2020; Foster et al., 2021; Mandelbaum et al., 2019). The presence of this conserved topography has led some to interpret BG circuits as *closed* loops but this view is at odds with the existence of cortico- cortical projections, the spread projection pattern of certain corticostriatal inputs and by the cross- talk between different loops that has been reported in the SNr/ SNc (Ambrosi & Lerner, 2022; Aoki et al., 2019; Haber et al., 2020; Harris & Sheperd, 2015; Hunnicutt et al., 2016). Overall, existing literature hints to at least some level of cross talk across parallel loops which are best described as *partially closed.*

Three principal loops have been proposed (Fig. 2). The limbic loop is implied in appetitive behavior and reinforcement and features limbic projections to the NAc including those from the medial prefrontal cortex (mPFC) (Lüscher & Janak, 2021; Voorn et al., 2004). The associative loop originates from medial associative cortices, prominently from the Orbitofrontal cortex (OFC) projecting to the DMS alongside with inputs from the basolateral amygdala (BLA) and is involved in the control of movement and goal- directed behaviors

(Graybiel & Grafton, 2015; Hart et al., 2014; Kupferschmidt et al., 2017; Nelson & Kreitzer, 2014; Redgrave et al., 2010; Yin & Knowlton, 2006). The sensorimotor loop originates from somatic sensorimotor cortices which project to the DLS and is involved in the control of movement and habitual behaviors (Graybiel & Grafton, 2015; Hart et al., 2014; Kupferschmidt et al., 2017; Nelson & Kreitzer, 2014; Redgrave et al., 2010; Yin & Knowlton, 2006).

The essential skeleton of striatal projections is similar across all loops, with similar contributions from dSPN and iSPN projections. Recent studies have started to investigate the structure of the associative and sensorimotor loops downstream of the striatum. One study found that ^{DMS}dSPNs and ^{DLS}dSPNs preferentially project to NPas1^{+} arkypallidal neurons, whereas ^{DMS}iSPNs and ^{DLS}iSPNs preferentially project to PV^{+} prototypic neurons in the GPe (Cui et al., 2021). Another study compared distinct PV^{+} GPe subpopulations projecting to the SNr and Pf finding that they received innervation from the DLS and DMS, respectively (Lilascharoen et al., 2021). These findings indicate that ^{PV}GPe neurons portion of the sensorimotor indirect pathway preferentially innervate the SNr, whereas ^{PV}GPe neurons portion of the associative indirect pathway preferentially innervate the Pf.

2.3 THE INPUT/ OUTPUT ORGANIZATION OF THE SNR

The SNr is mainly composed of GABAergic pacemaking projection neurons, with subpopulations of DAergic and GLUergic neurons that have also been described (Antal et al., 2014; Deniau et al., 2007). Early studies characterized SNr neurons for the expression of the calcium binding proteins PV or calretinin (CR) (Lee & Tepper, 2007). A second study classified SNr neurons for the expression of Vesicular GABA Transporter (VGAT) and PV finding subpopulations of VGAT^{+}/PV^{+} neurons, VGAT^{-}/PV^{+} neurons and VGAT^{+}/PV^{-} neurons (Rizzi & Tan, 2017). In this study, VGAT^{+} and PV^{+} neurons were found to project primarily to the CM thalamus and SNc, respectively. The activation of VGAT^{+} neurons impaired fine motor coordination, whereas the activation of PV^{+} neurons induced aversion (Rizzi & Tan, 2017). A third study found VGAT expression in the totality of SNr neurons and considered Glutamate Decarboxylase 2 (GAD2) as a marker, finding that most neurons were VGAT^{+}/ GAD2^{+}/ PV^{+}, with subpopulations of VGAT^{+}/ GAD2^{+}/ PV^{-} and VGAT^{+}/ GAD2^{-}/ PV^{+} also

present (McElvain et al., 2021). PV$^+$ neurons are enriched in the lateral portion of the SNr (Liu et al., 2020).

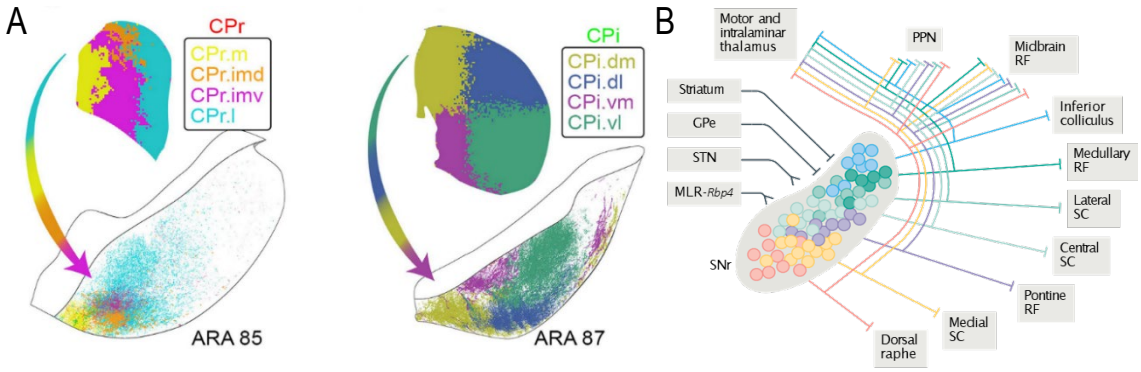

Figure 3: A): Organization of striatal inputs to the SNr. B): Organization of SNr outputs. Reprinted with permission from A) Foster et al., 2021; B) Arber & Costa 2022.

SNr neurons fire at high, regular rates in the slice independently of synaptic inputs (Atherton & Bevan, 2005). Their peculiar electrophysiological properties, including fast action potentials and high firing rates distinguish them from SNc dopaminergic neurons in slice preparations (Dupuis et al., 2015; McGregor et al., 2019). The intrinsic properties of SNr neurons vary based on their anatomical location and output connectivity (McElvain et al., 2021). It has been recently established that distinct subpopulations of SNr neurons project to different targets in the midbrain and brainstem, while collateralizing to innervate common targets which include the thalamus, the Pedunculopontine Nucleus (PPN) and the midbrain reticular formation (RF) (Deniau et al., 2007; McElvain et al., 2021; Lee et al., 2020; Liu et al., 2020). As summarized in figure 3, the specialized targets of SNr neurons vary along the medio-lateral axis. Further, SNr neurons innervated by the DMS and DLS maintain a medio-lateral topography on their common projection targets (Lee et al., 2020). Overall, functionally distinct subpopulations of SNr neurons broadcast signals to common thalamic and motor targets while innervating specialized targets.

PV$^+$ lateral SNr neurons and GAD2$^+$ medial SNr neurons have been studied in the context of sleep and movement (Liu et al., 2020). Whilst activation of both subpopulations increased movement termination, GAD2$^+$ neuron activation also induced sleep. Conversely, inhibition of GAD2$^+$ neurons reduced sleep and promoted movement initiation, whereas inhibition of PV$^+$ neurons suppressed movement termination. These results bear support to the idea that distinct subpopulations of SNr neurons are involved in motor control while also maintaining specialized functions.

SNr neurons integrate GABAergic direct pathway dSPN inputs and indirect pathway prototypic GPe inputs (Beier et al., 2017; Connelly et al., 2010; Mastro et al., 2014; Phillips et al., 2020). Further, NAc GABAergic inputs target the medial SNr (Aoki et al., 2019). The STN GLUergic inputs are also part of the indirect pathway (Deniau et al., 2007; Dupuis et al., 2015; Liu et al., 2020). Additional GLUergic inputs include a newly identified cortical input and the input from the Mesencephalic Locomotor Region (MLR) Retinol Binding Protein 4 (Rbp4) expressing neurons inputs (Ferreira-Pinto et al., 2021; Foster et al., 2021). It remains unclear whether SNr neurons portion of associative and sensorimotor basal ganglia loops differentially integrate distinct BG inputs.

3 BASAL GANGLIA CIRCUIT DYSFUNCTIONS

Understanding circuit dysfunctions underlying BG disorders is pivotal for the development of better treatments and the refinement of the existing ones. Further, studies of the diseased BG have refined our understanding of their normal function.

3.1 PARKINSON'S DISEASE

PD is a neurodegenerative disorder whose prevalence has been increasing worldwide during the past 30 years, with an estimate 8.5 million people living with PD in 2022 (Bloem et al., 2021; WHO, 2022). PD diagnosis is based on the presence of motor symptoms including bradykinesia, rigidity and tremor at rest responsive to L-DOPA or DBS (Postuma et al., 2015). Non motor symptoms including cognitive decline, depression and pain are also major contributors to disability in PD patients (Bloem et al., 2021). The emergence of motor symptoms is preceded by a prodromal phase lasting 10 years on average, characterized by symptoms including constipation, sleep disturbances, depression and hyposmia (Noyce et al., 2017).

A definitive diagnosis of PD can be only confirmed following post-mortem identification of pathological hallmarks which include degeneration of neuromelanin containing dopaminergic neurons, mainly in the SNc, and Lewy pathology. Lewy pathology is found primarily but not exclusively in the SNc,and can be also encountered in neurons that do not degenerate. Lewy pathology is characterized by accumulation of proteinaceous α-Synuclein aggregates in Lewy bodies and Lewy neurites, that also feature high-lipid content and crowding of dysmorphic mitochondria and other organelles around α-Synuclein aggregates (Shahmoradian et al., 2019; Wakabayashi et al., 2013).

In most PD cases dopaminergic neurodegeneration follows a slow and steady trajectory (Bloem et al., 2021). Motor symptoms become manifest when striatal dopamine content is reduced by more than 80% of normal (Ehringer & Hornykiewicz, 1960) and more than 45% of SNc DA neurons degenerate (Fearnley & Lees, 1991). Although prominent in the nigrostriatal pathway, neurodegeneration and Lewy pathology is also found in other regions of the CNS as well as in the autonomous and enteric nervous systems, indicating PD as a multisystemic disease (Klingelhoefer et al., 2017).

Monogenic causes explain 3-5% of PD cases, non-monogenic risk variant explain 16-36% of the cases, and the remainder is explained by an idiopathic origin (Bloem et al., 2021). The most common monogenic cause of PD is the *LRRK2* G2019S mutation which follows an autosomal dominant inheritance (Blauwendraat., 2020; Healy et al., 2008). The *LRRK2* gene (PARK8) encodes LRRK2 (dardarin), a large enzymatic protein with kinase and GTPase activity (Rocha et al., 2022). The *LRRK2* G2019S mutation results in an increased kinase activity which is thought to underlie its pathogenic effects (Leandrou et al., 2019). Endogenous *LRRK2* expression is found in striatal and cortical regions which receive inputs from and project to midbrain dopamine neurons, whereas lower expression is found in the midbrain (Skelton et al., 2022). The phenotype of patients carrying the *LRRK2* G2019S does differ from that of patients with idiopathic PD (Bloem et al., 2021). LRRK2 is a druggable target and the efficacy of LRRK2 kinase inhibitors is currently being assessed in clinical trials (Jennings et al., 2022; Rocha et al., 2022; Skelton et al., 2022).

Symptomatic but not disease modifying treatment options are currently available for PD. Motor symptoms respond in most cases to dopamine replacement therapy by administration of L-DOPA (Birkmayer & Hornykiewicz, 1961; Bloem et al., 2021; Carlsson et al., 1957). L-DOPA is the gold standard in PD therapy but its prolonged administration is complicated by the emergence of abnormal involuntary movements termed L-DOPA induced dyskinesias (Bezard et al., 2001). Deep brain stimulation (DBS) is also available wherein the response to pharmacological therapy becomes suboptimal (Hickey & Stacey, 2016; Limousin et al., 1995). The most common DBS target is the STN whose stimulation provides a good improvement of motor symptoms. Symptomatic therapies for PD act via restoring abnormal BG circuit function (Albin et al., 1989; Alexander & Crutcher, 1990; DeLong, 1990).

3.2 THE PARKINSONIAN BASAL GANGLIA

Cellular intrinsic changes, synaptic adaptations and firing abnormalities contribute to altered BG circuit function in PD (McGregor & Nelson, 2019; Shen et al., 2022; Wichmann, 2019).

Early studies detailing pathological changes in the parkinsonian BG were summarized in the classical model (Albin et al., 1989; Alexander & Crutcher, 1990; DeLong, 1990). This model posits that dopamine depletion induces bidirectional changes in the output produced by SPNs, which is then decreased? in dSPNs due to a reduction in the activation of excitatory D1 receptors and increased in iSPNs due to a reduction in the activation of inhibitory D2 receptors. This results in an over inhibition of the GPe and disinhibition of the GPi/ SNr. The resultant over inhibition of thalamic and cortical targets functionally explained the motor symptoms of PD. L-DOPA would act by reverting these circuit imbalances.

In line with the classic model, increased firing *rates* were identified in the STN and GPi in PD patients and non-human primate models of PD (Bergman et al., 1994; Benazzouz et al., 2002; Boraud et al., 1996; Boraud et al., 1998; Heimer et al., 200; Hutchinson et al., 1994). In addition, decreased firing rates were reported in the GPe, supporting the idea of a disinhibition of the indirect pathway, and in the motor cortex, supporting the idea of an over inhibition of the SNr/ GPi thalamic targets (Filion & Trembley, 1991; Heimer et al., 200; Hutchinson et al., 1994). However, firing rates in the SNr were found unaltered (Wichmann et al., 1991). Firing rates in the Ventral Anterior (VA) and Ventral Lateral (VL) thalamus were found unaltered in non-human primates but increased in PD patients (Molnar et al., 2005). Interventions aimed at decreasing the basal ganglia output via inactivation, surgical lesioning of the GPi/ SNr and inactivation, surgical lesioning or DBS of the STN have been successful in ameliorating motor symptoms in patients and animal models of PD (McGregor & Nelson, 2019; Wichmann, 2019). Taken together the predictions of the classical model are supported by inactivation studies and by changes of firing *rate* in the STN/ GPi/ SNr. However, the causality link between altered firing rates and abnormal BG output has been challenged by other lines of research. These lines focused in particular on the finding that (1) altered firing *patterns* and synchronization within neurons in the same BG region and across regions also occur and (2) the amplitude of local field potentials (LFP) across the BG is increased in the beta-band in PD patients and non-human primate models of PD (Bevan et al., 2002; Hammond et al., 2007; McGregor & Nelson, 2019; Wichmann, 2019).

The classic model predicts that BG circuit dysfunctions emerge from an increased iSPN output (Albin et al., 1989; Alexander & Crutcher, 1990; DeLong, 1990). This prediction has proven challenging to demonstrate definitively in PD patients (Singh et al., 2016; Valsky et al., 2020). Studies in animal models have reported either increases in the discharge rate of iSPNs, (Mallet et al., 2006; Sharott et al., 2017), imbalanced striatal output due to a decreased dSPN firing in PD mice (Ketzef et al., 2017; Maltese et al 2021; Ryan et al., 2018), restructuring of striatal

ensembles recruited by movement accompanied by decreased dSPN activity and increased iSPN activity at rest (Parker et al., 2018). These results converge in indicating that an altered striatal output emerges in animal models of PD. As acutely pointed out by Bergmann and colleagues (Valsky et al., 2020), even slight changes in striatal output might have profound impact on downstream BG nuclei. Whether this altered striatal output is causal for the changes observed throughout BG nuclei in PD remains unestablished.

PD is a multisystemic disease and even within the BG neurodegeneration of DA neurons does not only affect the nigrostriatal projection and the striatum, as relevant DA inputs, whose function remains poorly understood, are found in the GPe, GPi, STN and SNr (Shen et al., 2022). In this section, *in vivo* changes across the BG were reviewed. Increasing evidence indicates that synaptic adaptations and cell autonomous adaptations contribute to altering the function of all the major nuclei of the BG (Shen et al., 2022; Mallet et al., 2019). In the coming paragraph as well as in the results, discussion and **Papers 1-3** of this thesis, synaptic adaptations in PD mouse models will be discussed and examined in greater detail.

3.3 NMDA RECEPTORS AS PLAYERS AND TARGETS IN PD

Glutamate is the major excitatory neurotransmitter in the mammalian CNS whose actions depend on metabotropic (m-GluRs) and ionotropic (iGluRs) receptors (Traynelis et al., 2010). iGluRs include 4 different classes of receptors: amino-3-hydroxy-5-methyl-4-isoxazolepropionic acid (AMPA) receptors, kainate receptors, NMDA receptors, and Delta (GluD) receptors (Hansen et al., 2021). iGluRs are integral membrane assemblies of four multidomain subunits. iGluRs are generally permeable for K^+ and Na^+ but NMDARs and AMPA receptors lacking the GluA2 subunit are also permeable for Ca^{2+}. A distinguishing feature of NMDARs is the voltage-dependent block of their pore by Mg^{2+} ions at resting potential which is relieved at depolarized potentials (Paoletti et al., 2013).

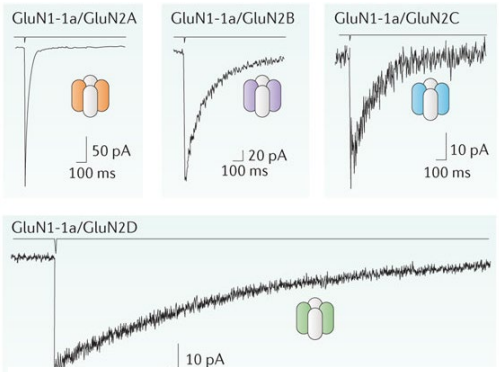

Figure 4: The subunit composition of the NMDARs influences their functional properties. Reprinted with permission from Paoletti et al., 2013

NMDARs are tetraheteromers formed by two obligatory GluN1 subunits that combine with two GluN2 (GluN2A, GluN2B, GluN2C, GluN2D) or GluN3 (GluN3A, GluN3B) subunits (Cull-Candy & Lezkiewicz, 2004; Hansen et al., 2021; Paoletti et al., 2013). The gating of NMDARs depends on the binding of two agonists: glycine, and glutamate (Kleckner et al., 1988). Glycine binds to the GluN1 subunits, the obligatory subunits for the formation of

functional NMDARs. Glutamate binds the GluN2 subunits whose expression in the CNS varies across development, across regions and within distinct cell types in the same region in the adult brain (Paoletti et al., 2013). The GluN3 subunits are glycine-binding and their role in the CNS has only just begun to be established (Otsu et al., 2019; Bossi et al., 2022). In the next paragraph, the properties of GluN2-containing NMDARs will be discussed.

The GluN2 content of NMDARs shapes their biophysical, pharmacological, and integrative properties (Hansen KB et al., 2021; Paoletti et al., 2013). Diheteromeric NMDARs contain two GluN1 and two identical GluN2 subunits and have been best characterized. The potency of glutamate binding on diheteromeric NMDARs is maximum on GluN2A- containing, lower on GluN2D-containing and intermediate on GluN2B/ C containing receptors. The deactivation kinetics of NMDARs are fast for GluN2A- containing (~40-50 ms), slow for GluN2D-containing (~4s) and intermediate for GluN2B/ C containing (~300-400 ms) receptors (Vicini et al., 1998; Wyllie et al., 1998). Ca^{2+} permeability and sensitivity to Mg^{2+} blockade are higher for GluN2A- and GluN2B- containing than on GluN2C/ 2D containing NMDARs (Qian et al., 2005; Retchless & Johnson, 2012). Specific allosteric modulators of diheteromeric NMDARs have allowed to study their function in specific behaviors and brain regions (Paoletti et al., 2013). Triheteromeric NMDARs are formed by the assembly of GluN1 with two distinct GluN2 subunits and possible combinations encountered in the CNS are GluN1/ 2A/ 2B, GluN1/2A/2C, GluN1/2B/2D (Hansen et al., 2021). The functional properties of triheteromeric NMDARs remain poorly understood also due to the lack of appropriate pharmacological tools for the investigation of their contribution to CNS synapses.

NMDARs are well poised to control signal integration in key nodes of the BG. Functional GluN2A and GluN2B-containing NMDARs are found in the adult SPNs (Durante et al., 2019; Li & Pozzo-Miller, 2019; Zhang et al., 2015). ChINs also express functional GluN2D-containing NMDARs (Tozzi et al., 2016; Zhang et al., 2014 (1); Zhang et al., 2014 (2)). GluN2B and GluN2D-containing NMDARs are expressed in STN neurons (Swanger et al., 2015), and GluN2B and GluN2D subunits are also found in SNr and SNc neurons (Suárez et al., 2010). *In vivo* firing of STN neurons was found to be decreased by the application of GluN2D antagonists and increased by the application of GluN2D agonists (Swanger et al., 2015). These studies indicate that GluN2B and GluN2D- containing NMDARs are involved in the control of signal integration and firing in critical BG regions.

Studies in animal models of PD have found altered NMDARs subunit composition. In the dorsal striatum of 6-OHDA lesioned mice, the SPN function of GluN2B- containing NMDARs was found to be reduced, whereas the function of GluN2D was increased. Further, a reduction

of GluN2D function in the parkinsonian state was observed in cholinergic interneurons (Zhang & Chergui., 2015). GluN2D function in cholinergic interneurons was found reduced in another study that used a α-Synuclein transgenic mouse model of PD (Tozzi et al., 2016). In the STN, a reduction in GluN2D expression has been reported in the MPTP model of PD in mice (Bhattacharya et al., 2017). Taken together, altered NMDAR subunit composition is observed in several nuclei of the BG in the parkinsonian state. NMDA receptors are involved in controlling synaptic plasticity. A study found that LTP induction, present in healthy mice, was impaired in 6-OHDA lesioned mice (Nouhi et al., 2017). Acute slice application of CIQ, a GluN2C/D positive allosteric modulator, rescued striatal LTP. Similarly, striatal LTP was rescued by acute treatment (1 day) or chronic treatment (7 days) with CIQ. Chronic CIQ treatment rescued forepaw use asymmetries in 6-OHDA lesioned mice.

The NMDA antagonists Amantadine and its derivative memantine are available for clinical use as monotherapy or as adjunct to multidrug treatment in PD. Amantadine can be used for the treatment of tremor and for the treatment of LID. The mild beneficial effects of amantadine and memantine are counteracted by their side effects. Targeting subunit-specific NMDA receptors might reduce the propensity of NMDAR antagonists to elicit side effects and ameliorate their therapeutic efficacy (Hallett and Standaert, 2004).

3.4 ALCOHOL AND THE BASAL GANGLIA

Neurocognitive disorders affecting the perceptual- motor and executive function domains emerge following acute alcohol intoxication and in AUD (*Diagnostic and Statistical Manual of the American Psychiatric Association V, DSM V, 2013)*. Altered BG circuit function contributes to key clinical symptoms including loss of control over alcohol intake, compulsions centered on alcohol and negative emotional states (Koob, 2021). Neurocognitive impairments are only partially recovered following prolonged abstinence (Shulte et al., 2014). Associative and sensorimotor BG loops have been investigated in animal models of AUD, considering their involvement in goal- directed and habitual action control (Gremel & Lovinger., 2017; Corbit & Janak., 2016).

Initial reinforcing effects of alcohol are thought to be dependent on increased dopamine release in the ventral and dorsal striatum (Di Chiara & Imperato, 1985; Mathews et al., 2006). Pivotal studies indicated that the emergence of habitual alcohol- seeking behavior was dependent on the DLS but not DMS (Corbit et al., 2012; Corbit et al., 2014). Acute ethanol application was shown to decrease GABAergic transmission in the DLS (Wilcox et al., 2014). In support to this finding, an optogenetic circuit study found that fast-spiking interneuron transmission onto

dorsal striatal SPNs was decreased by acute ethanol (Patton et al., 2016). In the putamen of alcohol drinking macaques, increased excitability and GLUergic transmission onto dorsal striatal SPNs and reduced GABAergic transmission were reported (Cuzon Carlson et al., 2011; Cuzon Carlson et al., 2018). Further, endocannabinoid (eCB)- dependent plasticity was found to be decreased on cortical inputs to the DLS (DePoy et al., 2013). Taken together, these changes indicate that alcohol might facilitate increased DLS output. However, it remains unclear how these changes contribute to altered action control and if the dSPN and iSPN projections are similarly affected.

Circuit changes in the DMS in rodent models of AUD have been investigated to a greater extent. Increased excitatory tone on ^{DMS}dSPNs paralleled by a decreased excitatory tone and increased inhibitory tone in ^{DMS}iSPNs was suggested to play a role in alcohol drinking behaviors (Cheng & Wang, 2019). Further, altered top- down control of DMS circuit function has also been implicated? in altered behavioral flexibility following sustained abstinence in rodents previously exposed to chronic ethanol vapor (CIE) or chronic drinking (Ma et al., 2021; Renteria et al., 2018; Renteria et al., 2021; Roltsch-Hellard et al., 2019). The OFC-DMS projection has been proposed to be central in the control of goal-directed behaviors and value-based decision making. OFC-DMS synapses were found to be weakened in the DMS of CIE mice (Renteria et al., 2018), due to increased CB1 receptor mediated inhibition (Renteria et al., 2021). These changes contributed to the excessive reliance of CIE mice on habitual action control. mPFC-DMS synapses have been involved in the cognitive control of action performance (de Kloet et al., 2021; Kupfershmidt et al., 2017). Altered plasticity at mPFC-DMS inputs has been implicated? in the control of alcohol- seeking behavior (Roltsch- Hellard et al., 2019).

These lines of research indicated profound effects of alcohol acute and chronic exposure in the striatum. However, little is known about the repercussions of these changes on downstream regions and how these changes affect the BG output.

4 AIMS

The overarching goal of this thesis was to identify the mechanisms underlying basal ganglia circuit dysfunctions in mouse models of PD and AUDs with a specific focus on the synaptic organization of the BG output.

Specific aims

1) To investigate if and how glutamatergic synapses and the subunit composition of NMDARare altered in the substantia nigra reticulata in the 6-OHDA model of Parkinson's disease and probe their role in motor dysfunctions (Study 1).

2) To assess if the overexpression of human LRRK2-G2019S in mice alters the functional properties and glutamatergic synapses of midbrain dopamine neurons and substantia nigra reticulata neurons (Studies 2 and 3).

3) To unravel the input organization and intrinsic properties of distinct neurons of the substantia nigra reticulata portion of associative and sensorimotor basal ganglia loops (Study 4).

4) To analyze if adaptations on the major inputs to the substantia nigra reticulata (striatal, pallidal, subthalamic) contribute to action control dysfunctions following chronic ethanol exposure (Study 4)

5) To detail the mechanisms of presynaptic modulation of striatal indirect pathway projections to the globus pallidus external segment by the G-Protein-Coupled-Receptors $GABA_B$ and CB1 (Study 5).

5 METHODOLOGICAL CONSIDERATIONS

At the hearth of the research work presented in this thesis lies the need to understand neural circuit organization and probe its role in the generation of behavior.

5.1 ETHICAL CONSIDERATIONS

The experimental work constituting this thesis relied on the use of mice as an experimental model. All the procedures were performed in compliance with the approved animal protocols at the Karolinska Institutet (Stockholm norra djurförsöksetiska nämn, 17018-2017 and 20464-2020) and at the National Institutes on Alcohol Abuse and Alcoholism (LIN-DL-1). The ”3R” principles of *replacement*, *reduction* and *refinement* were enforced throughout the entire duration of the studies. No alternative to the use of animals was found and the choice to conduct animal experiments was ethically motivated by the potential to alleviate human and animal suffering that experimental neuroscience bears. The brain circuitry analyzed in this thesis is preserved in its essential structure across mammals, therefore mouse models can allow to generate meaningful insights onto the basal ganglia function and its altered function in human disease to inform clinical translation (Grillner & Robertson, 2016). Finally, the availability and variety of transgenic mouse models that allow to model human disease and target neural circuits with great resolution is unmatched in other mammalian animal models.

5.2 THE 6-OHDA LESION MODEL OF PARKINSON’S DISEASE

The 6-OHDA lesion model is a neurotoxin- based model of PD that was initially developed in rats and later improved for its application in mice (Alvarez-Fischer et al., 2008; Grealish et al., 2010; Iwata et al., 2004; Lundblad et al., 2004; Ungerstedt et al., 1968; Thiele et al., 2012). The main rationale for the use of this model is the efficacy of 6-OHDA to induce fast catecholaminergic cell death, thus replicating the death of dopaminergic cells in the SNc and the loss of dopaminergic innervation of the striatum, major hallmarks in PD pathology. The 6-OHDA lesion model can be applied to produce different extents of DA depletion in the brain, with the final depletion levels depending on the dose, volume and site of injection used (Alvarez-Fischer et al., 2008; Boix et al., 2015; Grealish et al., 2010; Iwata et al., 2004; Lundblad et al., 2004; Masini et al., 2021; Thiele et al., 2012; Ungerstedt et al., 1968). The main limitation of this model is that it does not replicate two other major pathological hallmarks of PD, the progressive loss of SNc DA neurons and striatal DAergic innervation and the accumulation of Lewy bodies.

In **study 1**, we aimed at inducing a *unilateral full lesion* (>95% of striatal TH depletion) by injecting 6-OHDA in the medial forebrain bundle (MFB), a denervation extent that models human late-stage PD. Because of the limited 6-OHDA penetration across the blood-brain barrier and the potential of 6-OHDA to induce peripheral damage 6-OHDA injections are performed intracranially through stereotaxic surgery. The toxic effects of 6-OHDA on catecholaminergic neurons depend on the neurotoxin being transported inside DAergic and noradrenergic terminals through the dopamine (DAT) or noradrenaline (NAT) transporters, respectively (Simola et al., 2007). MAO-A oxidizes 6-OHDA releasing hydrogen peroxide that induces the production of reactive oxygen species, thus oxidative stress is the main mechanism of 6-OHDA induced neurotoxicity. Other mechanisms including mitochondrial damage have been proposed to mediate its effects (Simola et al., 1007; Jagmag et al., 2016).

One important aspect in the face validity of the 6-OHDA MFB unilateral lesion model is that it produces motor impairments including slow and reduced locomotion, spontaneous rotatory behavior ipsilateral to the injection site and motor asymmetries (Francardo et al., 2011; Heuer et al., 2012; Iancu et al., 2005; Thiele et al., 2012). Additionally, this model allows to avoid the use of DA agonist injection to reveal behavioral abnormalities. These drugs have the potential to induce plasticity changes through D1 receptors in SNr neurons or in striatal and subthalamic terminals in the SNr, thus confounding the interpretation of our results.

5.3 TRANSGENIC MOUSE MODEL OF HUMAN LRRK2*G2019S OVEREXPRESSION

Mutations in the LRRK2 gene are the most common genetic causes of PD. Among the possible mutations which have been studied in the LRRK2 gene, the most frequently identified is the G2019S mutation (Blauwendraat., 2020; Healy et al., 2008). This mutation induces an increased kinase activity of LRRK2 that results in higher susceptibility of DA neurons to cell death (Leandrou et al., 2019). LRRK2 is also expressed in other important nodes of the basal ganglia circuitry, including on cortical projection neurons and striatal SPNs (Skelton et al., 2022). Hence, genetic mouse models carrying a mutated LRRK2-G2019S represent an important tool to understand the pathophysiology of PD (Jagmag et al., 2015). LRRK2-G2019S rodent models have been generated by using knock-in (KI) and bacterial artificial chromosome (BAC) strategies. In **studies 2 and 3**, we have used a BAC mouse model of LRRK2-G2019S, using mice aged 10-12 months, an age that precedes the onset of overt neurodegeneration. In LRRK2-G2019S mice, neurodegeneration and motor phenotypes start to emerge in mice aged 12-16 months (Lim et al., 2018; Ramonet et al., 2011).

5.4 CHRONIC INTERMITTENT ETHANOL VAPOR EXPOSURE

Rodent models of acute and chronic alcohol exposure allow the investigation of systemic and organ-specific alcohol effects. Available models diverge for the delivery method (intragastric, intravenous, inhalation, oral) and schedules of ethanol administration. In **study 4**, a chronic intermittent ethanol (CIE) vapor exposure was used. CIE mimics 'binge-like' blood ethanol levels followed by periods of withdrawal, a pattern of alcohol intake observed in individuals with Alcohol Use Disorder (AUD) (Becker, 1994; Becker & Lopez, 2004; Griffin et al., 2009; Carvalho et al., 2019). In this schedule, I exposed mice to repeated cycles (4 cycles in our study, a total of 4 weeks) of ethanol vapor, each one consisting of 16 hours of exposure followed by 8 hours of withdrawal for 4 consecutive days, followed by 3 days of prolonged withdrawal. Control mice are exposed to air. The exposure begun 2 hours prior to the start of the dark cycle (between 5 and 6 pm). Mice were placed in separate vapor chambers, one of which was connected to a pump that continuously delivered ethanol vapor, while the other delivered air. Air flow was adjusted to produce vapor ethanol at concentrations of 0.160- 0.240 mg/L, measured using a breath analyzer. At the end of the first or second exposure of each cycle, I assessed circulating ethanol levels with an enzymatic assay assessed on tail-vein blood from a subgroup of mice. The goal of this exposure was to produce 'binge-like' ethanol levels, above 0.8 mg/dl, and ethanol vapor levels in the chambers were adjusted accordingly. In **study 5**, CIE mice were tested during prolonged withdrawal (>72h following the last exposure) to assess the neuronal deficits underlying impaired action execution (Renteria et al., 2018; Renteria et al., 2021).

5.5 WHOLE CELL PATCH CLAMP

Whole-cell patch clamp revolutionized neuroscience when it was developed more than 50 years ago, leading Erwin Neher and Bert Sakmann to the victory of the Nobel Prize in 1991 (Neher & Sakmann, 1976).

The patch-clamp technique was initially developed to obtain high quality, low-noise measurements of microscopic currents to resolve the properties of single ion channels. This occurred through the electrical isolation of a 'patch' of muscle cell membrane through a glass capillary (Neher & Sakmann, 1976). The technique was further refined to increase the seal resistance at the pipette-membrane interface to > 1GΩ allowing optimal insulation of the patch and increased signal-to-noise ratio, and finally matured into 3 distinct configurations: inside-out (the cytoplasmic side of the membrane is exposed outside of the patch), outside-out (the extracellular side of the membrane is exposed outside of the patch), and whole-cell (Sigworth & Neher, 1980; Hamill et al., 1981). The inside-out and outside-out configurations are obtained

by rupturing and separating the membrane patch from the cell after establishing a tight-seal and retracting the electrode and allow to probe the regulation of ion channel function by intracellular signaling molecules or extracellular ligands, respectively. The whole-cell configuration is obtained by rupturing a patch of membrane through the injection of negative pressure after establishing a >1GΩ seal and allows to access the inside of a whole cell electrically and physically through a low-resistance seal. The introduction of whole-cell patch clamp allowed to effectively study the functional properties of neurons and many other excitable or not excitable cells.

The versatility of this technique to being combined with an ever-growing landscape of tools to manipulate genes, cells and circuits allows its application to simultaneously examine brain function at multiple levels whilst maintaining its highest quality in the analysis of receptor function. Its applications span from cultured cells, acutely dissociated cells, brain organoids, acute brain slices to in vivo patch-clamp approaches.

In the simplest acute brain slice preparation, in which the cell types are not labeled using reporter genes or tracing methods, the experimenters access specific cell types based on their anatomical location and electrophysiological properties. The analysis of spontaneous or electrically-evoked neurotransmitter release allows the characterization of synaptic transmission. While some preparations allow to electrically stimulate only specific synaptic afferents (e.g. hippocampal Schaffer collaterals, cortico-striatal inputs by stimulation of the corpus callosum), in other brain regions this is not often possible. Despite this limitation, even a basic preparation combined with pharmacological manipulations remains extremely valuable to examine postsynaptic receptor function, presynaptic neurotransmitter release properties. Additionally, dye- based labeling of the recorded cells allow their post-hoc molecular identification. More advanced preparations allow for reporter-based or tracer-based identification of the studied cells and optogenetic stimulation of synaptic inputs to the cell. Both simple and more advanced preparations were used in the studies hereby presented.

In this thesis, three types of recordings were obtained:

1- Cell attached recordings: by establishing a ’loose-seal’ between the recording electrode and the membrane and recording in the voltage-clamp configuration. This method allows to measure action potential currents without disruptions of the intracellular milieu due to membrane rupturing and dialysis. This is the optimal method to study spontaneous neuronal firing activity.

2- Voltage-clamp recordings: this method was selected to measure currents evoked by ligand-gated ion channels, which included $GABA_A$ receptors, glutamate AMPA and NMDA receptors. The composition of the intracellular solution and the voltage command can be varied to isolate specific currents, and their identity can be further confirmed by applying specific antagonists. Notably, in **study 1** we used a pharmacological approach to dissect the subunit composition of NMDA receptors in the SNr. In **study 5** we used a similar pharmacological approach to identify the mechanisms of action of $GABA_B$ and CB1 receptors in the indirect pathway projections to the GPe.
3- Current-clamp recordings: in this configuration, spontaneous voltage fluctuations or voltage responses to current injections can be measured to determine the intrinsic membrane and action potential properties of a neuron. This modality reveals how the conductances active in each neuron act in concert to determine its excitability and its responses to synaptic inputs. In **study 4**, we used current-clamp recordings to identify the properties of regionally distinct SNr neurons and how they integrated striatal, pallidal and subthalamic inputs.

5.6 BEHAVIORAL METHODS TO PROBE ACTION CONTROL, ANXIETY AND LOCOMOTION IN MICE

Depending on the mouse model used and the experimental question, in this thesis various behavioral aspects were examined.

Open field test: mice are placed in a square or circular arena to analyze general kinetic parameters of their horizontal activity (locomotion) and vertical activity (rearings). In **study 1**, the horizontal activity of the 6-OHDA lesioned mouse model was analyzed to assess their parkinsonian-like hypolocomotor symptoms and perform inactivation experiments. In **study 2** a *de novo* behavioral characterization of the LRRK2-G2019S mouse line in the age range selected was performed. In addition to the basic parameters of mouse locomotion, anxiety-like traits were assessed by measuring the time spent in the periphery and center of the open field, as well rearings to assess exploratory behavior (Simon et al., 1994).

Light-dark box and elevated plus maze: these two tests assess anxiety-like traits by leveraging on the natural aversion of mice for open and bright spaces, respectively (Bourin & Hascoët, 2003). In the light-dark box test, mice explore an arena consisting for one third of a dark box, and two thirds of a light area. In **study 2** the number of entries on the light area and the total time spent in each compartment was analyzed. In the elevated plus maze, mice were allowed

to explore two closed arms and two open arms, and the total number of entries and time spent in the open arms was quantified.

Instrumental conditioning procedures: Instrumental conditioning operationally quantify the goal-directed and habitual properties of actions and have been widely used to analyze the contributions of the basal ganglia to action control (Balleine et al., 2007; Rossi & Yin, 2012). In instrumental conditioning paradigms, Action-Outcome (goal-directed) and Stimulus-Response (habitual) associations are established by pairing an action (e.g., lever press) with a rewarding outcome (e.g., sucrose pellet). These types of associations consolidate during instrumental training and their properties are tested with outcome devaluation procedures followed by brief extinction sessions (when outcome is not delivered). Outcome devaluation assesses the action-outcome properties of associative responding. The training schedule biases the animals towards goal-directed strategies or habitual strategies by using random ratio (RR, sensitive to outcome devaluation) or random interval schedules (RI, insensitive to outcome devaluation), respectively. Variations on the theme allow to also test for behavioral flexibility, motivation, learning and action kinematics. In the context of **study 5** we used a random ratio schedule to train CIE or AIR exposed mice and studied the effects of chronic alcohol exposure on action performance.

5.7 TRANSLATING SYNAPTIC MECHANISMS TO BEHAVIORAL PHENOTYPES: *IN VIVO* MANIPULATION STRATEGIES

The synaptic physiology experiments performed in studies 1 and 5 indicated novel mechanisms underlying basal ganglia circuit dysfunctions in mouse models of PD and chronic alcohol exposure. *In vivo* manipulations can be performed to understand the contribution of the proposed mechanism to *in vivo* phenotypes.

In **study 1**, intracranial microinjections of an NMDA receptor antagonist (DL-AP5) in the SNr were performed. This method allows to deliver a pharmacological agent to the brain and probe the role of the target receptor in a specific region on a given behavior, with the limitation that drug spillover onto neighboring regions might occur. Saline or DL-AP5 were injected and behavioral tests were repeated twice on each mouse with one day in between tests. Drug or saline injections were counterbalanced across days.

6 RESULTS

6.1 GLUTAMATERGIC ADAPTATIONS IN THE SNR IN A MOUSE MODEL OF PARKINSON'S DISEASE.

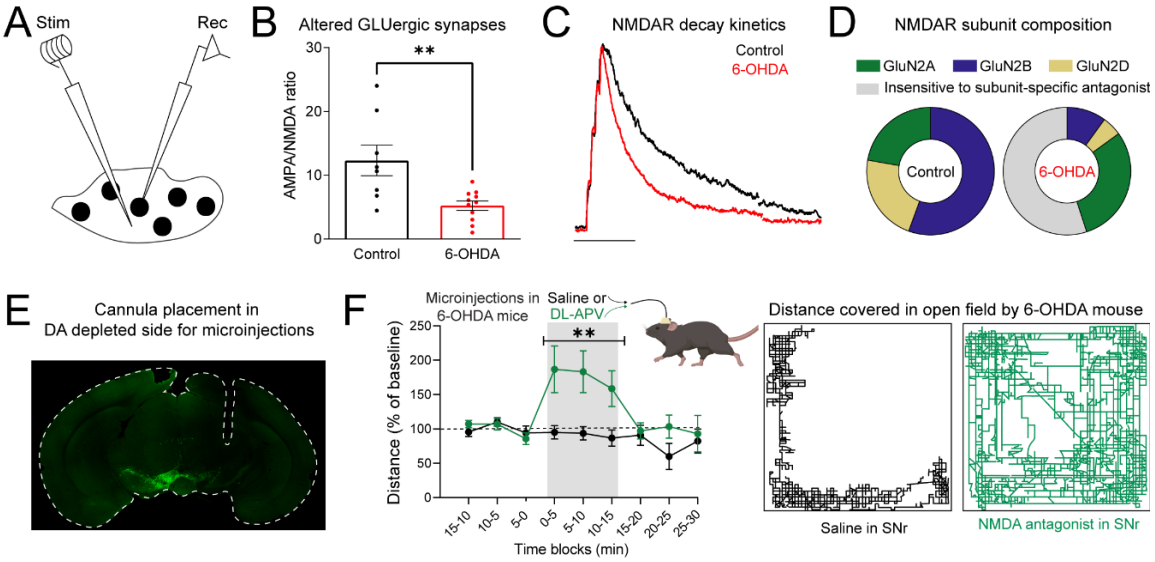

Fig 5; A: *A microelectrode was used to stimulate glutamate release in SNr slices and whole-cell voltage clamp was used to record post-synaptic AMPA and NMDAR mediated EPSCs.* B*: altered ratio between AMPA and NMDA-mediated currents in 6-OHDA mice.* C*: altered NMDA-EPSCs kinetics in 6-OHDA mice.* D*: altered NMDAR subunit composition in 6-OHDA mice, where the contribution of GluN2B and GluN2D was decreased.* E*: validation of cannula implants in 6-OHDA lesioned mice.* F*: time-course and representative tracks of distance covered during microinjections of DL-APV or saline in 6-OHDA mice.*

In **paper 1** we examined the glutamatergic synapses of the SNr in control and 6-OHDA lesioned mice. The SNr is a key node of the BG well positioned to control motor behaviors. It is generally assumed that increased firing of SNr neurons promotes movement cessation and decreased firing promotes movement initiation and maintenance. Synaptic inputs from the STN can increase SNr neuronal firing thus mediating movement suppression. Accordingly, inhibition of STN inputs to the SNr has been demonstrated to promote movement initiation in healthy conditions and rescue locomotor impairments in parkinsonian animal models. We focused on understanding whether altered glutamatergic transmission contributes to abnormal glutamatergic signaling in 6-OHDA lesioned mice. One caveat of these experiments was that by performing local stimulation of the slice additional inputs other that the STN inputs might also be recruited.

We first analyzed basic properties of glutamatergic synapses in the SNr. We recorded spontaneous and evoked AMPA- mediated EPSCs and found no difference in the frequency

and amplitude of spontaneous EPSCs and in the paired-pulse ration (PPR) of evoked EPSCs, indicating no changes in AMPA receptor function nor in parameters of presynaptic probability of glutamate release. Next, we assessed the relative contribution of NMDA receptors to glutamatergic synapses in the SNr by analyzing the AMPA/ NMDA ratio, a synaptic measure of experience-dependent or pathological plasticity in the CNS. We found that the AMPA/ NMDA ratio was decreased in SNr neurons of 6-OHDA mice. No change was identified in AMPA-mediated transmission in our initial experiments therefore our results can be summarized as an *increased relative contribution of NMDARs in GLUergic synapses of the SNr in 6-OHDA lesioned mice*.

We next characterized NMDAR function in the SNr of control and 6-OHDA lesioned mice. We compared the decay kinetics of NMDA-EPSCs in control and 6-OHDA mice and found that in 6-OHDA mice the NMDA-EPSCs decayed at a faster rate. This functional change pointed towards an altered NMDAR subunit composition in the SNr 6-OHDA lesioned. Using a pharmacological approach, we studied the contribution of different GluN2 (2A, 2B, 2D) subunits to NMDArs in the SNr of control and 6-OHDA lesioned mice. We found that diheteromeric NMDARs containing either GluN2A, GluN2B or GluN2D contributed to NMDAR-EPSCs in control mice. In 6-OHDA lesioned mice, we identified a reduction in the contribution of diheteromeric GluN2B- and GluN2D- containing NMDARs. Using immunohistochemistry and RNAscope, we evaluated the expression of GluN2A, GluN2B and *grin2d* in SNr neurons. We confirmed the expression of GluN2A, GluN2B and *grin2d* in SNr neurons, counter-validating our functional findings. The number of SNr neurons expressing GluN2A, GluN2B and *grin2d* was unaltered in the SNr of 6-OHDA lesioned mice. *Our findings indicate a reorganization of NMDARs in the SNr of 6-OHDA lesioned mice, with a decreased contribution of diheteromeric GluN2B and GluN2D containing NMDARs*. One possibility is that the relative contribution of triheteromeric NMDARs is increased in 6-OHDA lesioned mice while GluN2A-containing become the predominant diheteromeric NMDAR pool.

We finally tested whether NMDAR function in the SNr contributes to hypolocomotion in 6-OHDA lesioned mice. We used a microinjection strategy to acutely inhibit NMDAR-mediated transmission in the SNr while measuring spontaneous locomotion of 6-OHDA lesioned mice in the open field. Microinjections were performed in the SNr ipsilateral to the 6-OHDA lesion. We microinjected saline or saline + DL-AP5 (a pan- NMDAR antagonist) counterbalancing microinjections across mice and across days. We found that microinjections of DL-AP5 produced an increase in locomotion. Specifically, the distance covered and the locomotor speed

of 6-OHDA lesioned mice during the first 15 minutes following the microinjection were increased. These findings indicate that *inhibiting NMDAR signaling in the SNr contributes to rescue hypolocomotion in 6-OHDA lesioned mice*, an effect that might be due to a relieve of the tonically increased STN-SNr input postulated by the standard model.

Here, we identified a synaptic mechanism that alters glutamatergic input integration in the SNr via increased activity and altered subunit composition of NMDARs. Acute inhibition of NMDARs *in vivo* rescued hypolocomotion indicating that tonic NMDAR signaling contributes to the generation of PD-like motor impairments in 6-OHDA lesioned mice.

6.2 MIDBRAIN ADAPTATIONS INDUCED BY LRRK2 GENE MUTATIONS

The emergence of motor symptoms in PD is preceded by a prodromal phase whose underlying circuit mechanisms remain poorly understood. LRRK2-G2019S mice are a valuable tool to mechanistically investigate circuit dysfunctions induced by altered LRRK2 function in age ranges that precede overt neurodegeneration. In this study we performed molecular, behavioral, and electrophysiological analyses in mice overexpressing the mutated LRRK2-G2019S focusing on a middle age range (10-12 months old) during which neurodegeneration is not yet present.

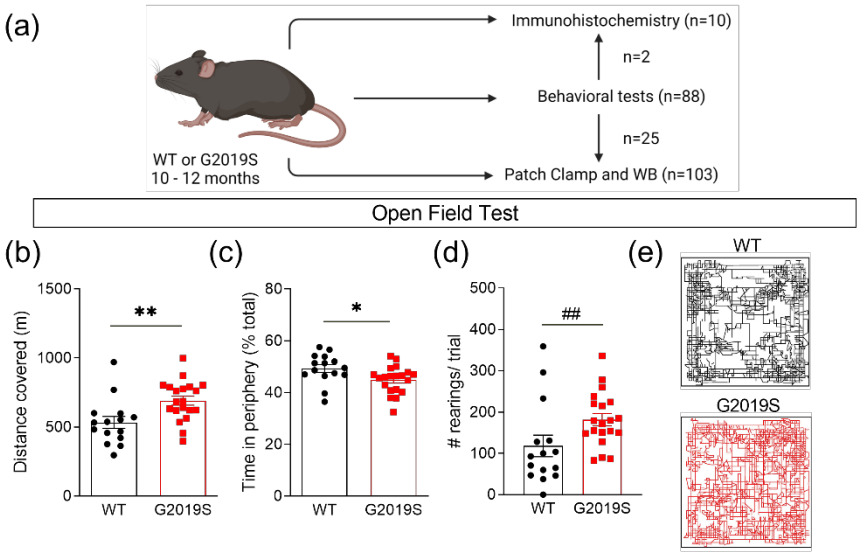

Figure 6: Increased exploratory behavior in LRRK2-G2019S mice. Adapted with permission from Skiteva et al., 2022

First, we assessed the dopaminergic systems in the brain by performing cell counts of TH expressing neurons in the SNc and VTA and found no difference between control and LRRK2-G2019S mice. Similarly, we did not detect changes in the expression of TH and of the dopamine transporter (DAT) in the striatum and nucleus accumbens. We next performed a

series of behavioral tests to investigate general locomotion, anxiety, and motor skills. *We found that mice carrying the LRRK2-G2019S mutation had increased locomotion and exploration compared to WT littermates*, but no anxiety-like behavior or motor coordination impairments (**Study 2**).

We focused our attention on midbrain DA neurons and found no difference in the firing frequency and pattern in SNc and VTA DA neurons (**Study 2**). Likewise, we did not detect alterations in the firing frequency and pattern of firing of SNr neurons, nor any change in the action potential properties of these neurons in LRRK2-G2019S mice compared to controls (**Study 3**).

We then analyzed glutamatergic synapses onto SNc dopamine neurons and found decreased probability of glutamate release and decreased frequency of spontaneous EPSCs, indicating presynaptic changes in glutamate release. No changes in the amplitude of spontaneous EPSCs or AMPA/ NMDA ratio in VTA neurons was identified. Importantly, these changes were acutely rescued by incubating the slices with a LRRK2 inhibitor demonstrating their dependency on altered LRRK2 function. Conversely, no changes in the presynaptic control of glutamate release or AMPA/NMDA ratio were observed in the VTA. The amplitude of AMPA-mediated spontaneous EPSCs was increased in the VTA of LRRK2-G2019S mice and these changes were reverted in slices incubated with a LRRK2 inhibitor (**Study 2**). Overall, *divergent changes in glutamatergic neurotransmission were observed in midbrain DA neurons of LRRK2 mice*.

In the SNr of LRRK2-G2019S mice, we found no change in the amplitude and frequency of spontaneous EPSCs, whereas a slight decrease in PPR indicated an increased probability of glutamate release. We also analyzed the decay kinetics of NMDA-EPSCs and the contribution of GluN2B to NMDARs in the SNr and found no difference in these parameters between control and LRRK2-G2019S mice (**Study 3**). Hence, in LRRK2 mice glutamatergic synapses in the SNr are altered through a presynaptic mechanism (**Study 3**).

Finally, we quantified the expression levels of glutamatergic synaptic markers in the midbrain and found decreased expression levels of the AMPA receptor subunit GluA1, NMDAR receptor subunit GluN1 and of the vesicular glutamate transporter 1 (VGLUT1) (**Study 2**).

Taken together, **studies 2 and 3** identified circuit alterations occurring in midbrain dopamine and GABA neurons of LRRK2-G2019S mice. Whilst the regularity of firing of SNc and VTA dopamine neurons and SNr GABA neurons was preserved, glutamatergic synapses were altered. Specifically, the probability of glutamate release was reduced in SNc neurons and

slightly increased in SNr neurons, whereas postsynaptic AMPA-mediated currents were increased in the VTA. The changes hereby reported occurred in an age range that preceded neurodegeneration and motor symptoms onset and indicate that *altered LRRK2 function impacts midbrain glutamatergic transmission in middle-aged mice*.

6.3 THE SYNAPTIC AND CIRCUIT ORGANIZATION OF THE SUBSTANTIA NIGRA PARS RETICULATA

The SNr is the major output region of the BG in rodents. A critical step in understanding the role of the basal ganglia in signal processing relevant to different behaviors and their contribution to brain-wide dynamics is to unravel their circuit and synaptic organization. The associative and sensorimotor basal ganglia loops control goal-directed and habitual behavior, respectively. In the first part of **study 4** we focused on the circuit organization of the associative and sensorimotor SNr.

Direct pathway inputs from the DMS and DLS define two distinct subregions of the SNr, spatially located in the medial and lateral portions of the nucleus, respectively. To study striatal inputs to the medial and lateral SNr, we used a viral approach to express the excitatory opsin Chronos in the DMS or DLS and performed whole-cell patch clamp recordings in SNr neurons. We confirmed the spatial location of DMS- connected neurons in the medial SNr and DLS-connected neurons in the lateral SNr. We studied the short-term plasticity properties of DMS-SNr projections and DLS-SNr projections and found that they were characterized by short-term depression and short-term facilitation, respectively. These results established presynaptic properties that differentiate the DMS-SNr and DLS-SNr projections. We next examined the molecular marker identity of DMS-targeted and DLS-targeted SNr neurons. PV-Cre mice were bred with mice carrying a 'floxed' Td-Tomato to selectively express the reporter in PV-expressing neurons. We recorded from PV-expressing (PV^+) and PV-not expressing (PV^-) neurons in mice transduced with Chronos in DMS or DLS. *We found that DLS- targeted SNr neurons were PV^+ whereas DMS- targeted SNr neurons were PV^-*.

Next, we characterized the firing properties of medial and lateral SNr neurons. Lateral SNr neurons had higher capacitance than medial SNr neurons, suggestive of a larger soma size. We observed no difference in the firing rate between medial and lateral SNr neurons. Medial neurons had wider action potentials (AP) and smaller afterhyperpolarization (AHP) compared to lateral SNr neurons. Medial SNr neurons had higher input resistance and higher rebound firing frequency than lateral neurons. Finally, medial SNr neurons had larger sag amplitude. We next asked if these electrophysiologically distinct SNr neuron subpopulations differentially

integrate striatal inputs. We found that *DMS and DLS inputs efficiently inhibited the firing of medial and lateral SNr neurons* in a frequency-dependent manner.

To study the GPe-SNr projection, we used PV-Cre mice to virally express Chronos in a Cre-dependent manner in PV^+ 'prototypic' GPe (^{PV}GPe) neurons. These cells have been identified as the SNr-projecting subpopulation of GPe neurons along with LHX6- expressing neurons which preferentially target the substantia nigra compacta (SNc). We found that the density of ^{PV}GPe terminals was higher in the lateral SNr. Using whole-cell patch clamp recordings to measure oIPSCs in the medial and lateral SNr, we found that oIPSC amplitude was larger in the lateral than in the medial SNr and found that both synapses were characterized by short-term depression. *Taken together, these findings indicate that the ^{PV}GPe projection is anatomically and functionally biased to the lateral SNr*.

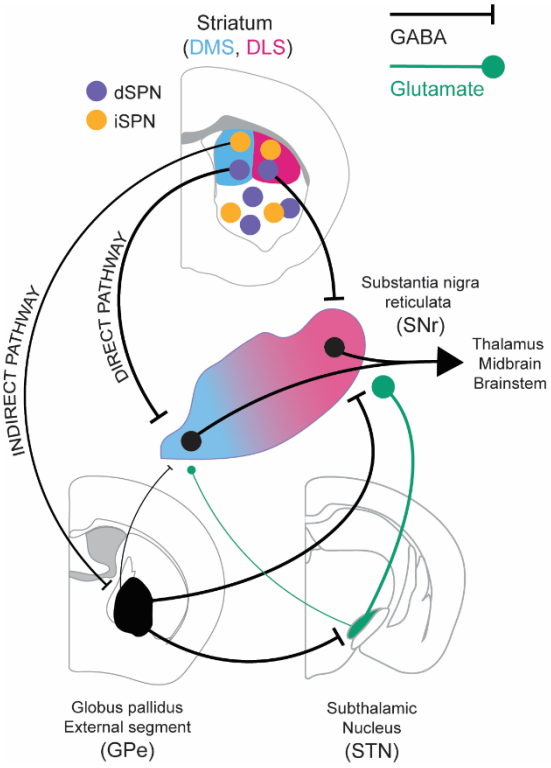

Figure 7: BG inputs to the SNr.

To study the STN-SNr projections, we used VGluT2-Cre mice to virally express a Cre-dependent version of Chronos in STN neurons. VGluT2 is a generic marker that labels the majority of STN neurons. We found that STN terminals were evenly distributed throughout the medio-lateral axis of the SNr. Next, we recorded oEPSCs in medial and lateral SNr neurons and found that the amplitude of oEPSCs was larger in lateral SNr neurons. STN-medial SNr and STN-lateral SNr projections also differed in their short-term plasticity, which indicated a higher probability of release at STN-lateral SNr than STN-medial SNr inputs. Finally, we analyzed the effects of STN projections on the firing of medial and lateral SNr neurons. We found that STN-SNr projections effectively increased the firing of medial and lateral SNr neurons. Taken together, these results indicate that *STN projections to the medial and lateral SNr have distinct functional properties*: STN-medial SNr projections are characterized by short-term facilitation and small oIPSCs but can effectively increase the firing of medial SNr neurons, due to their higher excitability; STN-lateral SNr projections are characterized by a slight short-term depression and large oIPSCs that effectively increase the firing of lateral SNr neurons.

The results illustrated in this section indicate that the associative and sensorimotor portions of the SNr are integrated in parallel loops that differ in their cell-type composition and BG input integration.

6.4 INPUT-SPECIFIC PLASTICITY ON DISTINCT BASAL GANGLIA OUTPUT SUBDOMAINS UNDERLIE ACTION CONTROL DYSFUNCTIONS FOLLOWING CHRONIC ETHANOL EXPOSURE

Acute and chronic alcohol consumption has profound effects on executive functions, action, and motor control. In the second part of **study 4**, we asked how striatal and cortico-striatal dysfunctions affect direct and indirect pathway projections to the SNr, and how these changes contribute to altered action control following chronic alcohol exposure.

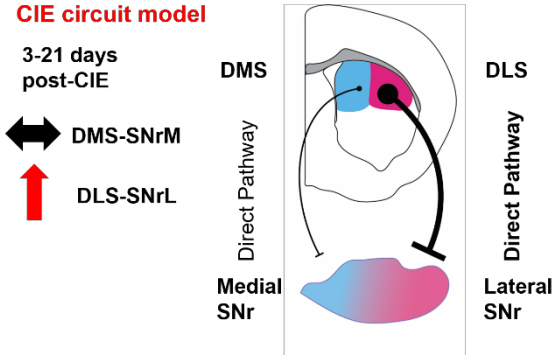

Figure 8: Plasticity of DLS-SNr inputs following chronic alcohol exposure.

By using the chronic intermittent ethanol (CIE) vapor exposure paradigm we first assessed striato-nigral and subthalamo-nigral synapses on the associative and sensorimotor SNr subdomains following chronic alcohol exposure. We found that DLS-SNr, but not DMS-SNr synapses were selectively potentiated following CIE, as measured by an increase in the frequency and amplitude of *quantal* IPSCs following optogenetic stimulation. Conversely, we found that the amplitude, paired-pulse ratios, and medio-lateral ratios of STN-SNr inputs to the medial and lateral SNr were unchanged following CIE. *Overall, we found that synapse- specific plasticity at DLS-SNr synapses is a novel circuit adaptation induced by chronic alcohol exposure.*

We next used an instrumental lever pressing task to assess action control following CIE. Mice were trained to press a single lever under a fixed ratio schedule of reinforcement, followed by a training on a random ratio schedule of reinforcement. AIR and CIE mice performance (head entries, rewards collected, licks, frequency of lever pressing) was similar during the fixed ratio training, indicating intact learning and motor performance in CIE mice. During random ratio training, we found that CIE mice performed the lever pressing task with a significantly higher rate of lever pressing compared to controls. *Taken together, these experiments indicate that CIE mice use different strategies for action performance in an instrumental lever pressing task.*

Overall, we demonstrate that ^{DLS}dSPN-SNr synapses are selectively potentiated following CIE. This synaptic mechanism might underlie altered action performance in CIE mice.

6.5 GPCRS CONTROL OF INDIRECT PATHWAY PROJECTIONS TO THE EXTERNAL GLOBUS PALLIDUS

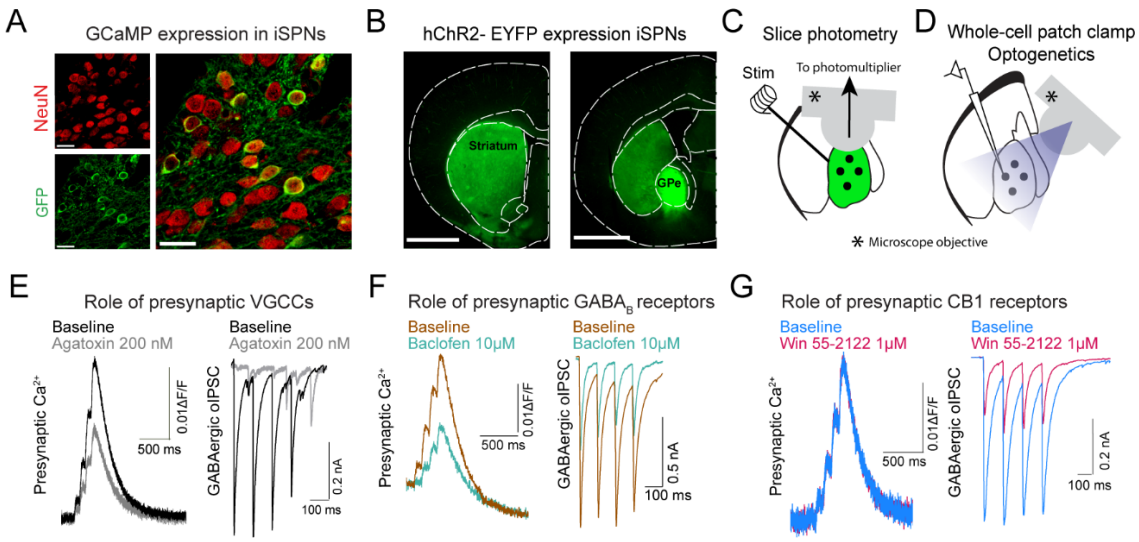

Figure 7: A: example micrographs of GCaMP expression in iSPNs. B: iSPN projections to the GPe in A2aCre-hChR2 mice. C: Schematic illustration of the setup for slice photometry recordings. D: Schematic illustration of the setup for whole-cell patch clamp combined with optogenetics recordings; E: P/Q type VGCCs inhibition reduced presynaptic calcium transients and GABA release on iSPN-GPe terminals. F: the $GABA_B$ receptor agonism reduced presynaptic calcium transients and GABA release at iSPN-GPe synapses. G: CB1 receptor agonism did not reduce presynaptic calcium transients while inhibiting GABA release at iSPN-GPe synapses.

The indirect pathway projections originate from striatal iSPNs, innervating the GPe. These projections participate in motor control and aversion processing and have classically been assigned an action-suppressing role. The iSPN-GPe projection represents only a fraction of the GABAergic input to the GPe, which also includes direct pathway 'bridge collateral' projections and local collaterals. As discussed in the Introduction of this thesis, presynaptic neuromodulation plays an important role in modulating the properties of a given synapse in the CNS. In study 4, we investigated the roles of two GPCRs on presynaptic calcium and neurotransmitter release specifically on the iSPN-GPe projections.

We used slice photometry to measure presynaptic calcium and patch-clamp electrophysiology to study neurotransmitter release. To selectively express the fluorescent calcium indicator GCaMP6f or the excitatory opsin hChR2 onto iSPNs, we crossed Adora2A-Cre (A2ACre) mice with mice carrying 'floxed' alleles for GCaMP6f of hChR2. To validate the strategy, we performed immunohistochemistry to quantify the percentage of striatal neurons expressing GCaMP6f in A2ACre-GCaMP6f mice and found that approximately 45% of striatal neurons

expressed GCaMP6f. These results agree with previously published ratios of striatal neuronal subtype composition. Further, using electrophysiology in A2aCre-hChR2 mice we found that optogenetic stimulation evoked only GABA release (oIPSCs) onto GPe neurons. These steps confirmed the validity of our strategy. Next, we found that the Presynaptic Calcium Transients (PreCaTs) measured with slice photometry and evoked through electrical stimulation of the slice were activity dependent, as their intensity scaled with stimulation intensity, and Ca^{2+} dependent, as their intensity was nearly null when extracellular Ca^{2+} was removed from the perfusion solution.

We first studied the Voltage- Gated Ca^{2+} -Channels (VGCC) subtypes mediating presynaptic Ca^{2+} and neurotransmitter release on the iSPN-GPe projections. In these experiments, after recording a stable baseline of PreCaTs or oIPSCs we bath- applied selective antagonists for specific VGCC subtypes. We found that P/Q type, but not N-type or L-type VGCCs mediated PreCaTs on the iSPN-GPe projections. We found that P/Q type VGCCs were the predominant VGCC mediating GABA release at iSPN-GPe synapses, but that N-type or L-type VGCCs also partially contributed to control GABA release.

Next, we studied the role of $GABA_B$ receptors on the iSPN-GPe projection. $GABA_B$ receptors were previously shown to control GABA release in the GPe, but their mechanisms of action at distinct synapses had not been detailed. Bath- application of a $GABA_B$ agonist significantly decreased the PreCaTs amplitude and the oIPSC amplitude, indicating that $GABA_B$ receptors control neurotransmitter release at the iSPN-GPe synapse through a VGCC-dependent mechanism.

Finally, we examined the role of CB1 receptors on the iSPN-GPe projection. CB1 receptors were shown to control GABA release in the GPe, but similarly to $GABA_B$ receptors their synaptic site of action and mechanism was not studied in detail. We found that the bath application of a CB1 agonist did not decrease PreCaTs amplitude. Conversely, bath application of a CB1 agonist significantly decreased oIPSCs amplitude. These results suggested that CB1 receptors might control neurotransmitter release at iSPN-GPe synapses through a VGCC-independent mechanism. We sought to test possible alternative targets that mediated CB1 inhibition of neurotransmitter release. We first recorded oIPSCs in presence of sodium voltage-gated channel (Na_V) and potassium voltage-gated channel-type 1 (K_V) antagonists and found that the effects of the CB1 agonist persisted under these conditions. Hence, CB1 effects at iSPN-GPe synapses appeared to be Na_V and K_V independent. Finally, we recorded mIPSCs, to focus on VGCC-independent neurotransmitter release. The bath application of the CB1 agonist decreased the frequency and amplitude of mIPSCs recorded under these conditions, indicating

that inhibition of neurotransmitter release at GABAergic synapses persisted when VGCC channels were blocked.

In summary, in study 4 we found that $GABA_B$ and CB1 receptors are key presynaptic modulators of the iSPN-GPe projection. The mechanisms of action of the two GPCRs are, however, distinct. $GABA_B$ receptors primarily control neurotransmitter release through the inhibition of presynaptic VGCCs, whereas CB1 receptors control neurotransmitter release through VGCC- independent mechanisms.

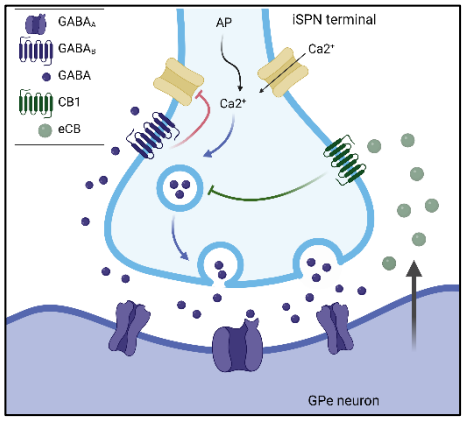

Figure 9: Mechanism of CB1 and $GABA_B$ control of iSPN-GPe projections

7 DISCUSSION AND FUTURE DIRECTIONS

This thesis examined the functional organization of basal ganglia circuits, their dysfunction in movement disorders and their contribution to altered action control following chronic ethanol exposure, by using an integrative approach that considered the receptor, synapse, circuit and behavior levels.

SNr circuit dysfunctions in animal models of PD: spotlight on glutamatergic synapses

In **study 1**, we identified a synaptic mechanism underlying altered glutamatergic input integration in SNr neurons. The change identified involved an increased relative contribution of NMDARs on SNr glutamatergic synapses and altered NMDAR subunit composition. **Study 1** advices that when pondering NMDARs as a pharmacological target for PD therapy, its subunit composition in key-brain regions for motor control such as the basal ganglia output shall be taken into account to guide the refinement of targeted approaches.

Two major limitations of the methods used must guide the careful interpretation of these results. By stimulating electrically the slice to evoke glutamate release, we could not identify in these experiment which synaptic inputs were being excited, therefore our findings apply to a 'generic' SNr glutamatergic synapse. Our pharmacological examination was limited by the lack of antagonists or allosteric modulators that target triheteromeric NMDARs. Our results invite future studies that consider the function of NMDARs at identified inputs to the SNr, as well as a detailed pharmacological analysis considering the role of tri-heteromeric NMDARs in the SNr in PD.

Plasticity of NMDARs subunit composition in animal models of PD contributes to pathophysiological changes observed in the striatum and STN (Bhattacharya et al., 2017; Tozzi et al., 2016; Zhang & Chergui., 2015). We found that acute application of an NMDAR antagonist in the SNr rescued hypolocomotion in 6-OHDA lesioned mice. These findings suggest a tonic activation of glutamatergic inputs to the SNr that has detrimental effects on motor output. Since these inputs signal through altered NMDARs, this might produce pathological effects on SNr neuronal firing via increased intracellular Ca^{2+} (Ibáñez-Sandoval et al., 2007). In the STN, another pacemaker region of the BG, NMDAR signaling has been found to participate to cell autonomous and synaptic aberrant adaptations affecting GPe-STN and hyperdirect projections in animal models of PD (Chu et al., 2015; Chu et al., 2017; McIver et al., 2019; Pan et al., 2014). A lesson from STN studies is that abnormal NMDAR signaling produces heterosynaptic adaptations. Intriguingly dSPN-SNr projections are potentiated in 6-OHDA lesioned mice (Borgkvist et al., 2015). Taken together, our results fit in a larger picture that places NMDARs as key regulators of circuit adaptations in DA-depleted states. Future studies shall expand the functional significance of the changes identified in our study.

The standard model predicts that an increased STN output activates the SNr. Our results are in agreement with this model, suggesting that decreasing glutamatergic input to the SNr has a prokinetic effect in parkinsonian mice. The SNr is involved in motor control via tonic inhibition of cortical output and of brainstem targets critical for the control of locomotion, including the PPN (Caggiano et al., 2018; Deniau et al., 2007; McElvain et al., 2021; Lee et al., 2020; Liu et al., 2020; Roseberry et al., 2016). It will be critical for future studies to identify the functional roles of diverse SNr projections for expanding the significance of an altered SNr output in PD. Considering the heterogeneity of SNr neurons on the basis of their output connectivity (McElvain et al., 2021) and molecular markers, it is possible that diverse cell- autonomous adaptations occur in distinct SNr subpopulations, differentially affecting distinct outputs.

In **studies 2 and 3**, we found that region-specific adaptations in glutamatergic synapses but not altered firing occur in VTA DA neurons, SNc DA neurons and SNr GABA neurons in a mouse model of human LRRK2-G2019S overexpression. The changes observed in the different synapses included increased and decreased probability of glutamate release in SNc and in SNr neurons, respectively, and decreased amplitude of postsynaptic AMPA-mediated currents in VTA neurons. We found that midbrain glutamatergic synapses are altered by LRRK2-G2019S, as the levels of GluN1, GluA1 and VGLUT1 in the midbrain of LRRK2-G2019S were reduced compared to their wild-type littermates. The most important conclusion is that LRRK2-G2019S modifies glutamatergic synapses in the midbrain prior to the onset of neurodegeneration.

Our findings indicate that the LRRK2-G2019S mutation has functional effects in the midbrain, although the expression levels of LRRK2 in this brain region are lower than those found in other BG regions (Skelton et al., 2022). In LRRK2-G2019S mice, neurodegeneration and motor phenotypes start to emerge in mice aged 12-16 months (Lim et al., 2018; Ramonet et al., 2011). However, behavioral alterations including altered reactivity to stressors, altered social behavior and anxiety-like phenotypes have been described in earlier age ranges where no neurodegeneration could be observed (Guevara et al., 2020; Lim et al., 2018; Matikainen-Ankney et al., 2018). These studies led to the investigation of the underlying circuit dysfunctions, which include altered glutamatergic transmission in the dorsal and ventral striatum and altered experience- dependent plasticity in response to acute and chronic social stress in the ventral striatum (Guevara et al., 2020; Lim et al., 2018; Matikainen-Ankney et al., 2018; Matikainen-Ankney et al., 2018). One possibility is that the changes we report might alter experience- dependent synaptic plasticity in midbrain neurons in response to environmental challenges and in response to aging.

The circuit organization of the associative and sensorimotor SNr

In **study 4,** we focused on the circuit organization of distinct subdomains of the SNr. Our initial interest was stimulated by clinical evidence and animal studies which indicated that altered action control in AUD results from BG circuit dysfunctions (Koob., 2021; Lovinger & Gremel., 2021). We focused on the associative and sensorimotor loops as habitual action control has been indicated as a predominant mode of behavioral control in AUD (Corbit & Janak, 2016).

First, we needed to establish the circuit properties of SNr neurons part of the ’associative’ and ’sensorimotor’ subdomains. It is important to clarify that the terminology used to define the two subdomains is based on their anatomical connectivity and on the view that the SNr is an output of both the associative and sensorimotor striatum. This definition is consistent with the parallel organization of basal ganglia loops, however a functional confirmation of the role of these distinct neuronal populations is still lacking. We used an optogenetic strategy to functionally study DMS-SNr and DLS-SNr circuits. Consistent with previous anatomical tracing studies, we found that medial SNr neurons received DMS inputs and lateral neurons received DLS inputs (Foster et al., 2021; Lee et al., 2020).

Our strategy allowed to address the presynaptic level of regulation of these projections, where we found that DMS- SNr inputs are characterized by short term depression/ high probability of release and DLS- SNr inputs are characterized by short term facilitation/ low probability of

release. Our DLS- SNr results are consistent with previous studies of striatonigral projections obtained using a sagittal slice preparation to stimulate the striatum and record in the SNr (Connelly et al., 2010). Our DMS- SNr results are not in line with this previous study likely due to a higher spatial selectivity of the optogenetic mapping method that we used (Connelly et al., 2010). These differences might underlie differential control of DMS- SNr and DLS- SNr projections by GPCRs including the CB1 receptor, since a medio- lateral expression gradient of expression has been previously reported (Davis et al., 2018). Future studies should clarify the origin of the differential presynaptic control of DMS-SNr and DLS-SNr projections.

We found that DLS- connected SNr neurons express PV, whereas DMS- connected SNr neurons are PV^-. Our results are consistent with the enrichment of PV^- expressing neurons in the lateral SNr (Liu et al., 2020; McElvain et al., 2021). Medial SNr neurons, on the contrary, have not been yet characterized based on the expression of a specific marker. Two studies indicated that PV^+ SNr neurons are involved in the control of movement initiation and maintenance, and fine motor control (Liu et al., 2020; Rizzi & Tan, 2019). Extending this finding to our circuit mapping, the functional role of PV^+ neurons seem consistent with their identification as sensorimotor neurons.

Our circuit mapping indicates that the lateral SNr is preferentially innervated by ^{PV}GPe neurons. These results are open to several interpretations. The first interpretation is based on the indication that ^{PV}GPe neurons represent the primary subpopulation of SNr projecting GPe neurons, as LHX6- expressing neurons have been reported to preferentially innervate the SNc (Evans et al., 2020; Mastro et al., 2014). Following this line of thought, our results might indicate that the GPe-SNr projection is biased to the lateral SNr where it contributes to motor control (Lilascharoen et al., 2021). It has been reported that DMS-targeted ^{PV}GPe neurons innervate the Pf and control reversal learning (Lilascharoen et al., 2021), indicating that the associative ^{PV}GPe projection might not primarily innervate the associative SNr. A third possibility is that a subpopulation of PV^- GPe neurons targets the medial SNr, although at the moment this remains a speculative possibility.

We found that the distribution of STN terminals was homogeneous across the SNr, however the amplitude of excitatory postsynaptic currents elicited was larger in the lateral than medial SNr. Consistent with a high excitability of medial SNr neurons, we found that the STN was capable of elevating SNr neuronal firing to a similar extent in both subpopulations. We also found that the presynaptic properties of STN projections to the medial and lateral SNr differed, being characterized by short-term facilitation and slight short-term depression, respectively. Overall, the STN inputs to the associative and sensorimotor SNr are differentially organized.

We found that the circuit organization of associative and sensorimotor SNr neurons follows distinct rules based of the input source and target cell type. Synaptic inputs from the ^{PV}GPe and STN are biased to the less excitable, larger and PV^+ sensorimotor neurons, which receive a strong projection from the DLS. Conversely, the highly excitable and PV^- associative SNr neurons receive a weaker synaptic input from the ^{PV}GPe and STN, whilst maintaining a strong synaptic input from the DMS. If STN inputs remain capable of exciting the firing of associative neurons our preliminary data suggest that this might not be the same for the inhibitory ^{PV}GPe input. A possibility is that this circuit architecture underlies a predominant control of the associative SNr by direct pathway inputs, whereas balanced direct/ indirect pathway inputs control the sensorimotor SNr. In other words, in the 'race' between direct and indirect pathways to control the basal ganglia output, the direct pathway might have a starting circuit advantage over the indirect pathway in the associative SNr (Schmidt et al., 2013).

Synapse- specific plasticity on the basal ganglia output following chronic ethanol exposure

The framework established in the first part of **study 4** allowed us to study the circuit dysfunctions underlying altered action control following chronic ethanol exposure. We tested synaptic inputs to the sensorimotor and associative SNr after exposing mice to 4 weeks of CIE. We found that STN inputs to the sensorimotor SNr where unchanged, whereas DLS inputs were potentiated in CIE exposed mice. Conversely, STN, and DMS inputs to the associative SNr remained unchanged in CIE exposed mice. On the basis of this synapse- specific plasticity, our findings indicate that the direct pathway input to the sensorimotor SNr becomes predominant following CIE.

The results of our synaptic screening can be applied in future studies to design a circuit- based intervention aimed at assessing the role of the DLS-SNr input in mediating altered action control in CIE mice. In our paradigm, we have observed that in an instrumental learning task CIE mice demonstrate altered action control during prolonged withdrawal. CIE mice performed an instrumental learning task by pressing at higher frequencies than AIR- exposed mice, a difference that might be due to altered movement kinematics and stop signal integration in the sensorimotor loop.

Control of indirect pathway projections to the GPe by GPCRs

In **study 5**, we focused on the presynaptic regulation of indirect pathway inputs to the GPe by the $GABA_B$ and CB1 receptors. $GABA_B$ receptors are thought to control the GPe microcircuitry through pre- and postsynaptic mechanisms (Kaneda & Kita, 2005). The

expression levels of CB1 receptors in the GPe are among the highest in the central nervous system due to the dense expression of these receptors on striatal inputs, and CB1 receptor agonists have been shown to exert catalepsy and ipsilateral rotations when locally infused in the GPe (Engler et al., 2006). As part of a broader effort to determine how presynaptic modulation contributes to basal ganglia circuit dynamics, we sought to determine how the CB1 and $GABA_B$ receptors control presynaptic Ca^{2+} and neurotransmitter release at iSPN-GPe projections. Our findings indicate a dissociation between CB1 and $GABA_B$ receptor signaling on iSPN-GPe terminals. CB1 receptors control GABA release at iSPN-GPe projections via VGCC- independent mechanisms, whereas $GABA_B$ receptors control GABA release at iSPN-GPe projections via inhibition of VGCC. One limitation of this study was that we could not identify the presynaptic target of CB1 receptors on iSPN-GPe terminals. Further, our analyses were mainly focalized on the presynaptic control of iSPN-GPe synapses and did not address important questions regarding the biological mechanisms through which the two receptors are recruited, or their relevance to distinct GPe sub-circuits.

8 ACKNOWLEDGEMENTS

This thesis wouldn't exist without the support of an exceptional group of people.

Karima, I will be forever grateful for the opportunity that you gave me. You infused me with a proactive attitude and taught me how to do hard experiments. All the way through, you've been graceful and fair. I've learned a lot. **Dave**. I was used to more formal environments when I heard you calling some dopamine neurons 'those guys'. Your curious and open attitude made me feel more at home in science. Thanks for supporting me. **Xiaoqun** thanks for the help to get me started in many procedures in the lab. **Per** it's been a pleasure collaborating with you in my first publication. Thanks **Jens** and **Andrea** for your precious mentoring.

Mona, you've been my first contact in Sweden, a guide during my first times in the lab and a caring friend outside. It means a lot. **Ning** you taught me how to remain calm under times of experimental uncertainty and got me through it with your faith in problem solving. **Olga**, after Sardinian and English now I know how to swear in Russian while patching. Rig friends will remain friends. **Giannis** it's been great sharing a project with you, I wish there were more. **Seba** your scientific acuity and enthusiasm for everything in life stepped the quality of my time in the US to a whole other level. **Pam** jumping from science to politics to Spanish to cats to movies made my US days flow so much easier. **Yolanda** I can't imagine the LIN without you, thank you for making me feel at home even when so far from home. A special thanks to **Alexa**, **Zev**, **Stephanie** for helping my projects during these last months and all other LIN folks.

There would be no Stockholm without my angels. **Alex** since day one we discussed openly and deeply about any topic and shared many great moments. **Branka** you've been a constant support and my cultural handbook to Sweden, Stockholm, and a lot more, including landlords. **Alessandro** thanks for all the fun times, the music and the Esa-sushis. Thanks to my **climbing crew** for entering in my life during these PhD years, it truly changed the game. **Carina**, what a lucky coincidence sharing climbing and science in two cities. It's been fun. Thanks **Luca R.**, **Sara**, **Luca G** for sharing a lot with me including the 'best pizza in Solna'.

Alle mie persone di sempre: senza di voi sarei uno sradicato. **Babbo**, **Mamma**, **Luca** il vostro affetto e' cio' che rende casa casa. **Costy, Wolfi** non vedo l'ora di fare il prossimo radical trip, e W grazie per avermi portato a Stoccolma la prima volta. Grazie a tutti gli **Olii** e a **Marco, Silvietta, Mari.** Vivubbi'. Le vostre visite hanno spesso portato il sole nella buia Svezia.

La cosa migliore che questi anni svedesi e americani mi hanno dato sei tu, **Giorgia.** Semplicemente grazie per tutto quello che stare assieme mi da.

9 REFERENCES

1. Abdi, A. *et al.* Prototypic and arkypallidal neurons in the dopamine-intact external globus pallidus. *J Neurosci* **35**, 6667–6688 (2015).
2. Abecassis, Z. A. *et al.* Npas1+-Nkx2.1+ Neurons Are an Integral Part of the Cortico-pallido-cortical Loop. *J Neurosci* **40**, 743–768 (2020).
3. Afsharpour, S. Topographical projections of the cerebral cortex to the subthalamic nucleus. *J Comp Neurol* **236**, 14–28 (1985).
4. Albin, R. L., Young, A. B. & Penney, J. B. The functional anatomy of basal ganglia disorders. *Trends Neurosci* **12**, 366–375 (1989).
5. Alexander, G. E. & Crutcher, M. D. Functional architecture of basal ganglia circuits: neural substrates of parallel processing. *Trends Neurosci* **13**, 266–271 (1990).
6. Alexander, G. E., DeLong, M. R. & Strick, P. L. Parallel organization of functionally segregated circuits linking basal ganglia and cortex. *Annu Rev Neurosci* **9**, 357–381 (1986).
7. Alvarez-Fischer, D. *et al.* Characterization of the striatal 6-OHDA model of Parkinson's disease in wild type and alpha-synuclein-deleted mice. *Exp Neurol* **210**, 182–193 (2008).
8. Ambrosi, P. & Lerner, T. N. Striatonigrostriatal circuit architecture for disinhibition of dopamine signaling. *Cell Rep* **40**, 111228 (2022).
9. American Psychiatric Association. *Diagnostic and Statistical Manual of Mental Disorders, Fifth edition*. (American Psychiatric Association, 2013).
10. Antal, M., Beneduce, B. M. & Regehr, W. G. The substantia nigra conveys target-dependent excitatory and inhibitory outputs from the basal ganglia to the thalamus. *J Neurosci* **34**, 8032–8042 (2014).
11. Aoki, S. *et al.* An open cortico-basal ganglia loop allows limbic control over motor output via the nigrothalamic pathway. *Elife* **8**, e49995 (2019).
12. Aristieta, A. *et al.* A Disynaptic Circuit in the Globus Pallidus Controls Locomotion Inhibition. *Curr Biol* **31**, 707-721.e7 (2021).
13. Atherton, J. F. & Bevan, M. D. Ionic mechanisms underlying autonomous action potential generation in the somata and dendrites of GABAergic substantia nigra pars reticulata neurons in vitro. *J Neurosci* **25**, 8272–8281 (2005).
14. Balleine, B. W. Animal models of action control and cognitive dysfunction in Parkinson's disease. in *Progress in Brain Research* vol. 269 227–255 (Elsevier, 2022).
15. Becker, H. C. Positive relationship between the number of prior ethanol withdrawal episodes and the severity of subsequent withdrawal seizures. *Psychopharmacology (Berl)* **116**, 26–32 (1994).
16. Becker, H. C. & Lopez, M. F. Increased ethanol drinking after repeated chronic ethanol exposure and withdrawal experience in C57BL/6 mice. *Alcohol Clin Exp Res* **28**, 1829–1838 (2004).
17. Beier, K. T. *et al.* Rabies screen reveals GPe control of cocaine-triggered plasticity. *Nature* **549**, 345–350 (2017).

18. Benazzouz, A. *et al.* Intraoperative microrecordings of the subthalamic nucleus in Parkinson's disease. *Mov Disord* **17 Suppl 3**, S145-149 (2002).

19. Bergman, H., Wichmann, T., Karmon, B. & DeLong, M. R. The primate subthalamic nucleus. II. Neuronal activity in the MPTP model of parkinsonism. *J Neurophysiol* **72**, 507–520 (1994).

20. Bevan, M. D., Magill, P. J., Terman, D., Bolam, J. P. & Wilson, C. J. Move to the rhythm: oscillations in the subthalamic nucleus-external globus pallidus network. *Trends Neurosci* **25**, 525–531 (2002).

21. Bhattacharya, S. *et al.* NMDA receptor blockade ameliorates abnormalities of spike firing of subthalamic nucleus neurons in a parkinsonian nonhuman primate. *J Neurosci Res* **96**, 1324–1335 (2018).

22. Blauwendraat, C., Nalls, M. A. & Singleton, A. B. The genetic architecture of Parkinson's disease. *Lancet Neurol* **19**, 170–178 (2020).

23. Bloem, B. R., Okun, M. S. & Klein, C. Parkinson's disease. *The Lancet* **397**, 2284–2303 (2021).

24. Boix, J., Padel, T. & Paul, G. A partial lesion model of Parkinson's disease in mice--characterization of a 6-OHDA-induced medial forebrain bundle lesion. *Behav Brain Res* **284**, 196–206 (2015).

25. Boraud, T., Bezard, E., Bioulac, B. & Gross, C. High frequency stimulation of the internal Globus Pallidus (GPi) simultaneously improves parkinsonian symptoms and reduces the firing frequency of GPi neurons in the MPTP-treated monkey. *Neurosci Lett* **215**, 17–20 (1996).

26. Boraud, T., Bezard, E., Guehl, D., Bioulac, B. & Gross, C. Effects of L-DOPA on neuronal activity of the globus pallidus externalis (GPe) and globus pallidus internalis (GPi) in the MPTP-treated monkey. *Brain Res* **787**, 157–160 (1998).

27. Borgkvist, A. *et al.* Loss of Striatonigral GABAergic Presynaptic Inhibition Enables Motor Sensitization in Parkinsonian Mice. *Neuron* **87**, 976–988 (2015).

28. Bossi, S. *et al.* GluN3A excitatory glycine receptors control adult cortical and amygdalar circuits. *Neuron* **110**, 2438-2454.e8 (2022).

29. Bourin, M. & Hascoët, M. The mouse light/dark box test. *European Journal of Pharmacology* **463**, 55–65 (2003).

30. Brittain, J.-S., Sharott, A. & Brown, P. The highs and lows of beta activity in cortico-basal ganglia loops. *Eur J Neurosci* **39**, 1951–1959 (2014).

31. Burke, D. A., Rotstein, H. G. & Alvarez, V. A. Striatal Local Circuitry: A New Framework for Lateral Inhibition. *Neuron* **96**, 267–284 (2017).

32. Caggiano, V. *et al.* Midbrain circuits that set locomotor speed and gait selection. *Nature* **553**, 455–460 (2018).

33. Carlsson, A., Lindqvist, M. & Magnusson, T. 3,4-Dihydroxyphenylalanine and 5-hydroxytryptophan as reserpine antagonists. *Nature* **180**, 1200 (1957).

34. Carvalho, A. F., Heilig, M., Perez, A., Probst, C. & Rehm, J. Alcohol use disorders. *The Lancet* **394**, 781–792 (2019).

35. Chang, H. T., Wilson, C. J. & Kitai, S. T. Single neostriatal efferent axons in the globus

pallidus: a light and electron microscopic study. *Science* **213**, 915–918 (1981).

36. Cheng, Y. & Wang, J. The use of chemogenetic approaches in alcohol use disorder research and treatment. *Alcohol* **74**, 39–45 (2019).

37. Chu, H.-Y., Atherton, J. F., Wokosin, D., Surmeier, D. J. & Bevan, M. D. Heterosynaptic regulation of external globus pallidus inputs to the subthalamic nucleus by the motor cortex. *Neuron* **85**, 364–376 (2015).

38. Chu, H.-Y., McIver, E. L., Kovaleski, R. F., Atherton, J. F. & Bevan, M. D. Loss of Hyperdirect Pathway Cortico-Subthalamic Inputs Following Degeneration of Midbrain Dopamine Neurons. *Neuron* **95**, 1306-1318.e5 (2017).

39. Chu, H.-Y., McIver, E. L., Kovaleski, R. F., Atherton, J. F. & Bevan, M. D. Loss of Hyperdirect Pathway Cortico-Subthalamic Inputs Following Degeneration of Midbrain Dopamine Neurons. *Neuron* **95**, 1306-1318.e5 (2017).

40. Connelly, W. M., Schulz, J. M., Lees, G. & Reynolds, J. N. J. Differential short-term plasticity at convergent inhibitory synapses to the substantia nigra pars reticulata. *J Neurosci* **30**, 14854–14861 (2010).

41. Corbit, L. H. & Janak, P. H. Habitual Alcohol Seeking: Neural Bases and Possible Relations to Alcohol Use Disorders. *Alcohol Clin Exp Res* **40**, 1380–1389 (2016).

42. Corbit, L. H., Nie, H. & Janak, P. H. Habitual alcohol seeking: time course and the contribution of subregions of the dorsal striatum. *Biol Psychiatry* **72**, 389–395 (2012).

43. Corbit, L. H., Nie, H. & Janak, P. H. Habitual responding for alcohol depends upon both AMPA and D2 receptor signaling in the dorsolateral striatum. *Front Behav Neurosci* **8**, 301 (2014).

44. Crittenden, J. R. & Graybiel, A. M. Basal Ganglia Disorders Associated with Imbalances in the Striatal Striosome and Matrix Compartments. *Front. Neuroanat.* **5**, (2011).

45. Cui, Q. *et al.* Striatal Direct Pathway Targets Npas1+ Pallidal Neurons. *J Neurosci* **41**, 3966–3987 (2021).

46. Cull-Candy, S. G. & Leszkiewicz, D. N. Role of distinct NMDA receptor subtypes at central synapses. *Sci STKE* **2004**, re16 (2004).

47. Cuzon Carlson, V. C., Grant, K. A. & Lovinger, D. M. Synaptic adaptations to chronic ethanol intake in male rhesus monkey dorsal striatum depend on age of drinking onset. *Neuropharmacology* **131**, 128–142 (2018).

48. Cuzon Carlson, V. C. *et al.* Synaptic and morphological neuroadaptations in the putamen associated with long-term, relapsing alcohol drinking in primates. *Neuropsychopharmacology* **36**, 2513–2528 (2011).

49. Davis, M. I. *et al.* The cannabinoid-1 receptor is abundantly expressed in striatal striosomes and striosome-dendron bouquets of the substantia nigra. *PLoS One* **13**, e0191436 (2018).

50. de Kloet, S. F. *et al.* Bi-directional regulation of cognitive control by distinct prefrontal cortical output neurons to thalamus and striatum. *Nat Commun* **12**, 1994 (2021).

51. Deffains, M. *et al.* Subthalamic, not striatal, activity correlates with basal ganglia downstream activity in normal and parkinsonian monkeys. *Elife* **5**, e16443 (2016).

52. DeLong, M. R. Primate models of movement disorders of basal ganglia origin. *Trends Neurosci* **13**, 281–285 (1990).

53. Deniau, J. M., Mailly, P., Maurice, N. & Charpier, S. The pars reticulata of the substantia nigra: a window to basal ganglia output. *Prog Brain Res* **160**, 151–172 (2007).

54. DePoy, L. *et al.* Chronic alcohol produces neuroadaptations to prime dorsal striatal learning. *Proc Natl Acad Sci U S A* **110**, 14783–14788 (2013).

55. Di Chiara, G. & Imperato, A. Ethanol preferentially stimulates dopamine release in the nucleus accumbens of freely moving rats. *Eur J Pharmacol* **115**, 131–132 (1985).

56. Dudman, J. T. & Krakauer, J. W. The basal ganglia: from motor commands to the control of vigor. *Curr Opin Neurobiol* **37**, 158–166 (2016).

57. Dupuis, J. P. *et al.* Dopamine-dependent long-term depression at subthalamo-nigral synapses is lost in experimental parkinsonism. *J Neurosci* **33**, 14331–14341 (2013).

58. Durante, V. *et al.* Alpha-synuclein targets GluN2A NMDA receptor subunit causing striatal synaptic dysfunction and visuospatial memory alteration. *Brain* **142**, 1365–1385 (2019).

59. Ehringer, H. & Hornykiewicz, O. [Distribution of noradrenaline and dopamine (3-hydroxytyramine) in the human brain and their behavior in diseases of the extrapyramidal system]. *Klin Wochenschr* **38**, 1236–1239 (1960).

60. Engler, B., Freiman, I., Urbanski, M. & Szabo, B. Effects of Exogenous and Endogenous Cannabinoids on GABAergic Neurotransmission between the Caudate-Putamen and the Globus Pallidus in the Mouse. *J Pharmacol Exp Ther* **316**, 608–617 (2006).

61. Evans, R. C. *et al.* Functional Dissection of Basal Ganglia Inhibitory Inputs onto Substantia Nigra Dopaminergic Neurons. *Cell Rep* **32**, 108156 (2020).

62. Fearnley, J. M. & Lees, A. J. Ageing and Parkinson's disease: substantia nigra regional selectivity. *Brain* **114 (Pt 5)**, 2283–2301 (1991).

63. Féger, J., Bevan, M. & Crossman, A. R. The projections from the parafascicular thalamic nucleus to the subthalamic nucleus and the striatum arise from separate neuronal populations: a comparison with the corticostriatal and corticosubthalamic efferents in a retrograde fluorescent double-labelling study. *Neuroscience* **60**, 125–132 (1994).

64. Ferreira-Pinto, M. J. *et al.* Functional diversity for body actions in the mesencephalic locomotor region. *Cell* **184**, 4564-4578.e18 (2021).

65. Ferrier, D. *The Functions of the brain*. (Smith, Elder, & Co, London, 1876).

66. Fife, K. H. *et al.* Causal role for the subthalamic nucleus in interrupting behavior. *Elife* **6**, e27689 (2017).

67. Filion, M. & Tremblay, L. Abnormal spontaneous activity of globus pallidus neurons in monkeys with MPTP-induced parkinsonism. *Brain Res* **547**, 142–151 (1991).

68. Floresco, S. B. The nucleus accumbens: an interface between cognition, emotion, and action. *Annu Rev Psychol* **66**, 25–52 (2015).

69. Foster, N. N. *et al.* The mouse cortico-basal ganglia-thalamic network. *Nature* **598**,

188–194 (2021).

70. Francardo, V. *et al.* Impact of the lesion procedure on the profiles of motor impairment and molecular responsiveness to L-DOPA in the 6-hydroxydopamine mouse model of Parkinson's disease. *Neurobiol Dis* **42**, 327–340 (2011).

71. Gerfen, C. R. The neostriatal mosaic: multiple levels of compartmental organization. *Trends Neurosci* **15**, 133–139 (1992).

72. Gerfen, C. R. *et al.* D1 and D2 dopamine receptor-regulated gene expression of striatonigral and striatopallidal neurons. *Science* **250**, 1429–1432 (1990).

73. Giovanniello, J. *et al.* A Central Amygdala-Globus Pallidus Circuit Conveys Unconditioned Stimulus-Related Information and Controls Fear Learning. *J Neurosci* **40**, 9043–9054 (2020).

74. Gittis, A. H. *et al.* New roles for the external globus pallidus in basal ganglia circuits and behavior. *J Neurosci* **34**, 15178–15183 (2014).

75. Graybiel, A. M. & Grafton, S. T. The striatum: where skills and habits meet. *Cold Spring Harb Perspect Biol* **7**, a021691 (2015).

76. Grealish, S., Mattsson, B., Draxler, P. & Björklund, A. Characterisation of behavioural and neurodegenerative changes induced by intranigral 6-hydroxydopamine lesions in a mouse model of Parkinson's disease. *Eur J Neurosci* **31**, 2266–2278 (2010).

77. Gremel, C. M. & Lovinger, D. M. Associative and sensorimotor cortico-basal ganglia circuit roles in effects of abused drugs. *Genes Brain Behav* **16**, 71–85 (2017).

78. Griffin, W. C., Lopez, M. F. & Becker, H. C. Intensity and duration of chronic ethanol exposure is critical for subsequent escalation of voluntary ethanol drinking in mice. *Alcohol Clin Exp Res* **33**, 1893–1900 (2009).

79. Grillner, S. & Robertson, B. The Basal Ganglia Over 500 Million Years. *Curr Biol* **26**, R1088–R1100 (2016).

80. Guevara, C. A. *et al.* LRRK2 mutation alters behavioral, synaptic, and nonsynaptic adaptations to acute social stress. *J Neurophysiol* **123**, 2382–2389 (2020).

81. Haber, S. N., Fudge, J. L. & McFarland, N. R. Striatonigrostriatal pathways in primates form an ascending spiral from the shell to the dorsolateral striatum. *J Neurosci* **20**, 2369–2382 (2000).

82. Haber, S. Perspective on basal ganglia connections as described by Nauta and Mehler in 1966: Where we were and how this paper effected where we are now. *Brain Res* **1645**, 4–7 (2016).

83. Hallett, P. J. & Standaert, D. G. Rationale for and use of NMDA receptor antagonists in Parkinson's disease. *Pharmacol Ther* **102**, 155–174 (2004).

84. Hamill, O. P., Marty, A., Neher, E., Sakmann, B. & Sigworth, F. J. Improved patch-clamp techniques for high-resolution current recording from cells and cell-free membrane patches. *Pflugers Arch* **391**, 85–100 (1981).

85. Hammond, C., Bergman, H. & Brown, P. Pathological synchronization in Parkinson's disease: networks, models and treatments. *Trends Neurosci* **30**, 357–364 (2007).

86. Hansen, K. B. *et al.* Structure, Function, and Pharmacology of Glutamate Receptor Ion Channels. *Pharmacol Rev* **73**, 298–487 (2021).

87. Harris, K. D. & Shepherd, G. M. G. The neocortical circuit: themes and variations. *Nat Neurosci* **18**, 170–181 (2015).

88. Healy, D. G. *et al.* Phenotype, genotype, and worldwide genetic penetrance of LRRK2-associated Parkinson's disease: a case-control study. *Lancet Neurol* **7**, 583–590 (2008).

89. Heimer, G., Bar-Gad, I., Goldberg, J. A. & Bergman, H. Dopamine replacement therapy reverses abnormal synchronization of pallidal neurons in the 1-methyl-4-phenyl-1,2,3,6-tetrahydropyridine primate model of parkinsonism. *J Neurosci* **22**, 7850–7855 (2002).

90. Hernández, V. M. *et al.* Parvalbumin+ Neurons and Npas1+ Neurons Are Distinct Neuron Classes in the Mouse External Globus Pallidus. *J Neurosci* **35**, 11830–11847 (2015).

91. Heuer, A., Smith, G. A., Lelos, M. J., Lane, E. L. & Dunnett, S. B. Unilateral nigrostriatal 6-hydroxydopamine lesions in mice I: motor impairments identify extent of dopamine depletion at three different lesion sites. *Behav Brain Res* **228**, 30–43 (2012).

92. Hickey, P. & Stacy, M. Deep Brain Stimulation: A Paradigm Shifting Approach to Treat Parkinson's Disease. *Front Neurosci* **10**, 173 (2016).

93. Higgs, M. H., Jones, J. A., Chan, C. S. & Wilson, C. J. Periodic unitary synaptic currents in the mouse globus pallidus during spontaneous firing in slices. *J Neurophysiol* **125**, 1482–1500 (2021).

94. Hintiryan, H. *et al.* The mouse cortico-striatal projectome. *Nat Neurosci* **19**, 1100–1114 (2016).

95. Hunnicutt, B. J. *et al.* A comprehensive excitatory input map of the striatum reveals novel functional organization. *Elife* **5**, e19103 (2016).

96. Hutchison, W. D. *et al.* Differential neuronal activity in segments of globus pallidus in Parkinson's disease patients. *Neuroreport* **5**, 1533–1537 (1994).

97. Iancu, R., Mohapel, P., Brundin, P. & Paul, G. Behavioral characterization of a unilateral 6-OHDA-lesion model of Parkinson's disease in mice. *Behav Brain Res* **162**, 1–10 (2005).

98. Ibáñez-Sandoval, O. *et al.* Bursting in Substantia Nigra Pars Reticulata Neurons In Vitro: Possible Relevance for Parkinson Disease. *Journal of Neurophysiology* **98**, 2311–2323 (2007).

99. Iwata, S., Nomoto, M., Morioka, H. & Miyata, A. Gene expression profiling in the midbrain of striatal 6-hydroxydopamine-injected mice. *Synapse* **51**, 279–286 (2004).

100. Jagmag, S. A., Tripathi, N., Shukla, S. D., Maiti, S. & Khurana, S. Evaluation of Models of Parkinson's Disease. *Front Neurosci* **9**, 503 (2015).

101. Jahanshahi, M., Obeso, I., Rothwell, J. C. & Obeso, J. A. A fronto-striato-subthalamic-pallidal network for goal-directed and habitual inhibition. *Nat Rev Neurosci* **16**, 719–732 (2015).

102. Jennings, D. *et al.* Preclinical and clinical evaluation of the LRRK2 inhibitor DNL201 for Parkinson's disease. *Sci Transl Med* **14**, eabj2658 (2022).

103. Kaneda, K. & Kita, H. Synaptically Released GABA Activates Both Pre- and Postsynaptic GABA B Receptors in the Rat Globus Pallidus. *Journal of Neurophysiology* **94**, 1104–1114 (2005).

104. Ketzef, M. & Silberberg, G. Differential Synaptic Input to External Globus Pallidus Neuronal Subpopulations In Vivo. *Neuron* **109**, 516-529.e4 (2021).

105. Ketzef, M. *et al.* Dopamine Depletion Impairs Bilateral Sensory Processing in the Striatum in a Pathway-Dependent Manner. *Neuron* **94**, 855-865.e5 (2017).

106. Kish, S. J., Shannak, K. & Hornykiewicz, O. Uneven pattern of dopamine loss in the striatum of patients with idiopathic Parkinson's disease. Pathophysiologic and clinical implications. *N Engl J Med* **318**, 876–880 (1988).

107. Kita, T. & Kita, H. The subthalamic nucleus is one of multiple innervation sites for long-range corticofugal axons: a single-axon tracing study in the rat. *J Neurosci* **32**, 5990–5999 (2012).

108. Kita, T., Osten, P. & Kita, H. Rat subthalamic nucleus and zona incerta share extensively overlapped representations of cortical functional territories. *J Comp Neurol* **522**, 4043–4056 (2014).

109. Kleckner, N. W. & Dingledine, R. Requirement for glycine in activation of NMDA-receptors expressed in Xenopus oocytes. *Science* **241**, 835–837 (1988).

110. Koob, G. F. Drug Addiction: Hyperkatifeia/Negative Reinforcement as a Framework for Medications Development. *Pharmacol Rev* **73**, 163–201 (2021).

111. Kuhar, M. J., Pert, C. B. & Snyder, S. H. Regional distribution of opiate receptor binding in monkey and human brain. *Nature* **245**, 447–450 (1973).

112. Kupferschmidt, D. A., Juczewski, K., Cui, G., Johnson, K. A. & Lovinger, D. M. Parallel, but Dissociable, Processing in Discrete Corticostriatal Inputs Encodes Skill Learning. *Neuron* **96**, 476-489.e5 (2017).

113. Leandrou, E. *et al.* Kinase activity of mutant LRRK2 manifests differently in hetero-dimeric vs. homo-dimeric complexes. *Biochem J* **476**, 559–579 (2019).

114. Lee, C. R. & Tepper, J. M. Morphological and physiological properties of parvalbumin- and calretinin-containing gamma-aminobutyric acidergic neurons in the substantia nigra. *J Comp Neurol* **500**, 958–972 (2007).

115. Lee, J., Wang, W. & Sabatini, B. L. Anatomically segregated basal ganglia pathways allow parallel behavioral modulation. *Nat Neurosci* **23**, 1388–1398 (2020).

116. Lévesque, M. & Parent, A. The striatofugal fiber system in primates: a reevaluation of its organization based on single-axon tracing studies. *Proc Natl Acad Sci U S A* **102**, 11888–11893 (2005).

117. Li, W. & Pozzo-Miller, L. Differences in GluN2B-Containing NMDA Receptors Result in Distinct Long-Term Plasticity at Ipsilateral versus Contralateral Cortico-Striatal Synapses. *eNeuro* **6**, ENEURO.0118-19.2019 (2019).

118. Lilascharoen, V. *et al.* Divergent pallidal pathways underlying distinct Parkinsonian behavioral deficits. *Nat Neurosci* **24**, 504–515 (2021).

119. Lim, J. *et al.* LRRK2 G2019S Induces Anxiety/Depression-like Behavior before the Onset of Motor Dysfunction with 5-HT1A Receptor Upregulation in Mice. *J Neurosci* **38**, 1611–1621 (2018).

120. Limousin, P. *et al.* Bilateral subthalamic nucleus stimulation for severe Parkinson's disease. *Mov Disord* **10**, 672–674 (1995).

121. Liu, D. *et al.* A common hub for sleep and motor control in the substantia nigra. *Science* **367**, 440–445 (2020).

122. Lovinger, D. M. & Gremel, C. M. A Circuit-Based Information Approach to Substance Abuse Research. *Trends Neurosci* **44**, 122–135 (2021).

123. Lundblad, M., Picconi, B., Lindgren, H. & Cenci, M. A. A model of L-DOPA-induced dyskinesia in 6-hydroxydopamine lesioned mice: relation to motor and cellular parameters of nigrostriatal function. *Neurobiol Dis* **16**, 110–123 (2004).

124. Mallet, N., Delgado, L., Chazalon, M., Miguelez, C. & Baufreton, J. Cellular and Synaptic Dysfunctions in Parkinson's Disease: Stepping out of the Striatum. *Cells* **8**, E1005 (2019).

125. Mallet, N. *et al.* Dichotomous organization of the external globus pallidus. *Neuron* **74**, 1075–1086 (2012).

126. Maltese, M., March, J. R., Bashaw, A. G. & Tritsch, N. X. Dopamine differentially modulates the size of projection neuron ensembles in the intact and dopamine-depleted striatum. *eLife* **10**, e68041 (2021).

127. Mandelbaum, G. *et al.* Distinct Cortical-Thalamic-Striatal Circuits through the Parafascicular Nucleus. *Neuron* **102**, 636-652.e7 (2019).

128. Masini, D. & Kiehn, O. Targeted activation of midbrain neurons restores locomotor function in mouse models of parkinsonism. *Nat Commun* **13**, 504 (2022).

129. Masini, D. *et al.* A Guide to the Generation of a 6-Hydroxydopamine Mouse Model of Parkinson's Disease for the Study of Non-Motor Symptoms. *Biomedicines* **9**, 598 (2021).

130. Mastro, K. J., Bouchard, R. S., Holt, H. A. K. & Gittis, A. H. Transgenic mouse lines subdivide external segment of the globus pallidus (GPe) neurons and reveal distinct GPe output pathways. *J Neurosci* **34**, 2087–2099 (2014).

131. Mathews, T. A., John, C. E., Lapa, G. B., Budygin, E. A. & Jones, S. R. No role of the dopamine transporter in acute ethanol effects on striatal dopamine dynamics. *Synapse* **60**, 288–294 (2006).

132. Matikainen-Ankney, B. A. *et al.* Parkinson's Disease-Linked LRRK2-G2019S Mutation Alters Synaptic Plasticity and Promotes Resilience to Chronic Social Stress in Young Adulthood. *J Neurosci* **38**, 9700–9711 (2018).

133. McElvain, L. E. *et al.* Specific populations of basal ganglia output neurons target distinct brain stem areas while collateralizing throughout the diencephalon. *Neuron* **109**, 1721-1738.e4 (2021).

134. McGregor, M. M. *et al.* Functionally Distinct Connectivity of Developmentally Targeted Striosome Neurons. *Cell Rep* **29**, 1419-1428.e5 (2019).

135. Miyamoto, Y. & Fukuda, T. New Subregions of the Mouse Entopeduncular Nucleus Defined by the Complementary Immunoreactivities for Substance P and Cannabinoid Type-1 Receptor Combined with Distributions of Different Neuronal Types. *eNeuro* **9**, ENEURO.0208-22.2022 (2022).

136. Molnar, G. F., Pilliar, A., Lozano, A. M. & Dostrovsky, J. O. Differences in neuronal firing rates in pallidal and cerebellar receiving areas of thalamus in patients with Parkinson's disease, essential tremor, and pain. *J Neurophysiol* **93**, 3094–3101 (2005).

137. Naito, A. & Kita, H. The cortico-pallidal projection in the rat: an anterograde tracing study with biotinylated dextran amine. *Brain Res* **653**, 251–257 (1994).

138. Nauta, W. J. & Mehler, W. R. Projections of the lentiform nucleus in the monkey. *Brain Res* **1**, 3–42 (1966).

139. Neher, E. & Sakmann, B. Single-channel currents recorded from membrane of denervated frog muscle fibres. *Nature* **260**, 799–802 (1976).

140. Nelson, A. B. & Kreitzer, A. C. Reassessing models of basal ganglia function and dysfunction. *Annu Rev Neurosci* **37**, 117–135 (2014).

141. Nouhi, M., Zhang, X., Yao, N. & Chergui, K. CIQ, a positive allosteric modulator of GluN2C/D-containing N-methyl-d-aspartate receptors, rescues striatal synaptic plasticity deficit in a mouse model of Parkinson's disease. *CNS Neurosci Ther* **24**, 144–153 (2018).

142. Otsu, Y. *et al.* Control of aversion by glycine-gated GluN1/GluN3A NMDA receptors in the adult medial habenula. *Science* **366**, 250–254 (2019).

143. Pamukcu, A. *et al.* Parvalbumin+ and Npas1+ Pallidal Neurons Have Distinct Circuit Topology and Function. *J Neurosci* **40**, 7855–7876 (2020).

144. Pan, M.-K. *et al.* Deranged NMDAergic cortico-subthalamic transmission underlies parkinsonian motor deficits. *J Clin Invest* **124**, 4629–4641 (2014).

145. Paoletti, P., Bellone, C. & Zhou, Q. NMDA receptor subunit diversity: impact on receptor properties, synaptic plasticity and disease. *Nat Rev Neurosci* **14**, 383–400 (2013).

146. Parker, J. G. *et al.* Diametric neural ensemble dynamics in parkinsonian and dyskinetic states. *Nature* **557**, 177–182 (2018).

147. Patton, M. H., Roberts, B. M., Lovinger, D. M. & Mathur, B. N. Ethanol Disinhibits Dorsolateral Striatal Medium Spiny Neurons Through Activation of A Presynaptic Delta Opioid Receptor. *Neuropsychopharmacology* **41**, 1831–1840 (2016).

148. Phillips, R. S., Rosner, I., Gittis, A. H. & Rubin, J. E. The effects of chloride dynamics on substantia nigra pars reticulata responses to pallidal and striatal inputs. *Elife* **9**, e55592 (2020).

149. Postuma, R. B. *et al.* MDS clinical diagnostic criteria for Parkinson's disease. *Mov Disord* **30**, 1591–1601 (2015).

150. Qian, A., Buller, A. L. & Johnson, J. W. NR2 subunit-dependence of NMDA receptor channel block by external Mg2+. *J Physiol* **562**, 319–331 (2005).

151. Rajakumar, N., Elisevich, K. & Flumerfelt, B. A. Parvalbumin-containing GABAergic neurons in the basal ganglia output system of the rat. *J Comp Neurol* **350**, 324–336 (1994).

152. Ramonet, D. *et al.* Dopaminergic neuronal loss, reduced neurite complexity and autophagic abnormalities in transgenic mice expressing G2019S mutant LRRK2. *PLoS One* **6**, e18568 (2011).

153. Redgrave, P. *et al.* Goal-directed and habitual control in the basal ganglia: implications for Parkinson's disease. *Nat Rev Neurosci* **11**, 760–772 (2010).

154. Renteria, R., Baltz, E. T. & Gremel, C. M. Chronic alcohol exposure disrupts top-down control over basal ganglia action selection to produce habits. *Nat Commun* **9**, 211 (2018).

155. Renteria, R. *et al.* Mechanism for differential recruitment of orbitostriatal transmission during actions and outcomes following chronic alcohol exposure. *Elife* **10**, e67065 (2021).

156. Rizzi, G. & Tan, K. R. Synergistic Nigral Output Pathways Shape Movement. *Cell Rep* **27**, 2184-2198.e4 (2019).

157. Rocha, E. M., Keeney, M. T., Di Maio, R., De Miranda, B. R. & Greenamyre, J. T. LRRK2 and idiopathic Parkinson's disease. *Trends in Neurosciences* **45**, 224–236 (2022).

158. Roltsch Hellard, E. *et al.* Optogenetic control of alcohol-seeking behavior via the dorsomedial striatal circuit. *Neuropharmacology* **155**, 89–97 (2019).

159. Roseberry, T. K. *et al.* Cell-Type-Specific Control of Brainstem Locomotor Circuits by Basal Ganglia. *Cell* **164**, 526–537 (2016).

160. Rossi, M. A. & Yin, H. H. Methods for studying habitual behavior in mice. *Curr Protoc Neurosci* **Chapter 8**, Unit-8.29 (2012).

161. Ryan, M. B., Bair-Marshall, C. & Nelson, A. B. Aberrant Striatal Activity in Parkinsonism and Levodopa-Induced Dyskinesia. *Cell Reports* **23**, 3438-3446.e5 (2018).

162. Saunders, A. *et al.* A direct GABAergic output from the basal ganglia to frontal cortex. *Nature* **521**, 85–89 (2015).

163. Schmidt, R., Leventhal, D. K., Mallet, N., Chen, F. & Berke, J. D. Canceling actions involves a race between basal ganglia pathways. *Nat Neurosci* **16**, 1118–1124 (2013).

164. Schulte, M. T. & Hser, Y.-I. Substance Use and Associated Health Conditions throughout the Lifespan. *Public Health Rev* **35**, https://web-beta.archive.org/web/20150206061220/http://www.publichealthreviews.eu/upload/pdf_files/14/00_Schulte_Hser.pdf (2014).

165. Schweizer, N. *et al.* Reduced Vglut2/Slc17a6 Gene Expression Levels throughout the Mouse Subthalamic Nucleus Cause Cell Loss and Structural Disorganization Followed by Increased Motor Activity and Decreased Sugar Consumption. *eNeuro* **3**, ENEURO.0264-16.2016 (2016).

166. Serra, G. P., Guillaumin, A., Baufreton, J., Georges, F. & Wallén-Mackenzie, Å. *Aversion encoded in the subthalamic nucleus*. http://biorxiv.org/lookup/doi/10.1101/2020.07.09.195610 (2020).

167. Shabel, S. J., Proulx, C. D., Piriz, J. & Malinow, R. Mood regulation. GABA/glutamate co-release controls habenula output and is modified by antidepressant treatment. *Science* **345**, 1494–1498 (2014).

168. Sharott, A., Vinciati, F., Nakamura, K. C. & Magill, P. J. A Population of Indirect Pathway Striatal Projection Neurons Is Selectively Entrained to Parkinsonian Beta Oscillations. *J. Neurosci.* **37**, 9977–9998 (2017).

169. Shen, W., Zhai, S. & Surmeier, D. J. Striatal synaptic adaptations in Parkinson's disease. *Neurobiol Dis* **167**, 105686 (2022).

170. Siegler Retchless, B., Gao, W. & Johnson, J. W. A single GluN2 subunit residue controls NMDA receptor channel properties via intersubunit interaction. *Nat Neurosci* **15**, 406–413, S1-2 (2012).

171. Sigworth, F. J. & Neher, E. Single Na+ channel currents observed in cultured rat muscle cells. *Nature* **287**, 447–449 (1980).

172. Silberberg, G. & Bolam, J. P. Local and afferent synaptic pathways in the striatal microcircuitry. *Curr Opin Neurobiol* **33**, 182–187 (2015).

173. Simola, N., Morelli, M. & Carta, A. R. The 6-hydroxydopamine model of Parkinson's disease. *Neurotox Res* **11**, 151–167 (2007).

174. Simon, P., Dupuis, R. & Costentin, J. Thigmotaxis as an index of anxiety in mice. Influence of dopaminergic transmissions. *Behav Brain Res* **61**, 59–64 (1994).

175. Singh, A. *et al.* Human striatal recordings reveal abnormal discharge of projection neurons in Parkinson's disease. *Proc. Natl. Acad. Sci. U.S.A.* **113**, 9629–9634 (2016).

176. Skelton, P. D., Tokars, V. & Parisiadou, L. LRRK2 at Striatal Synapses: Cell-Type Specificity and Mechanistic Insights. *Cells* **11**, 169 (2022).

177. Stephenson-Jones, M. *et al.* A basal ganglia circuit for evaluating action outcomes. *Nature* **539**, 289–293 (2016).

178. Suárez, F. *et al.* Functional heterogeneity of NMDA receptors in rat substantia nigra pars compacta and reticulata neurones. *Eur J Neurosci* **32**, 359–367 (2010).

179. Swanger, S. A. *et al.* NMDA Receptors Containing the GluN2D Subunit Control Neuronal Function in the Subthalamic Nucleus. *J Neurosci* **35**, 15971–15983 (2015).

180. Thiele, S. L., Warre, R. & Nash, J. E. Development of a unilaterally-lesioned 6-OHDA mouse model of Parkinson's disease. *J Vis Exp* 3234 (2012) doi:10.3791/3234.

181. Tooley, J. *et al.* Glutamatergic Ventral Pallidal Neurons Modulate Activity of the Habenula-Tegmental Circuitry and Constrain Reward Seeking. *Biol Psychiatry* **83**, 1012–1023 (2018).

182. Tozzi, A. *et al.* Alpha-Synuclein Produces Early Behavioral Alterations via Striatal Cholinergic Synaptic Dysfunction by Interacting With GluN2D N-Methyl-D-Aspartate Receptor Subunit. *Biol Psychiatry* **79**, 402–414 (2016).

183. Traynelis, S. F. *et al.* Glutamate receptor ion channels: structure, regulation, and function. *Pharmacol Rev* **62**, 405–496 (2010).

184. Tritsch, N. X. & Sabatini, B. L. Dopaminergic modulation of synaptic transmission in cortex and striatum. *Neuron* **76**, 33–50 (2012).

185. Ungerstedt, U. 6-Hydroxy-dopamine induced degeneration of central monoamine neurons. *Eur J Pharmacol* **5**, 107–110 (1968).

186. van der Kooy, D. & Carter, D. A. The organization of the efferent projections and striatal afferents of the entopeduncular nucleus and adjacent areas in the rat. *Brain Res* **211**, 15–36 (1981).

187. Vicini, S. *et al.* Functional and pharmacological differences between recombinant N-methyl-D-aspartate receptors. *J Neurophysiol* **79**, 555–566 (1998).

188. Wallén-Mackenzie, Å. *et al.* Spatio-molecular domains identified in the mouse subthalamic nucleus and neighboring glutamatergic and GABAergic brain structures.

Commun Biol **3**, 338 (2020).

189. Watson, G. D. R. *et al.* Thalamic projections to the subthalamic nucleus contribute to movement initiation and rescue of parkinsonian symptoms. *Sci Adv* **7**, eabe9192 (2021).

190. Weglage, M. *et al. Sst+ GPi output neurons provide direct feedback to key nodes of the basal ganglia and drive behavioral flexibility*. http://biorxiv.org/lookup/doi/10.1101/2022.03.16.484460 (2022).

191. Wichmann, T. *et al.* Comparison of MPTP-induced changes in spontaneous neuronal discharge in the internal pallidal segment and in the substantia nigra pars reticulata in primates. *Exp Brain Res* **125**, 397–409 (1999).

192. Wichmann, T. Changing views of the pathophysiology of Parkinsonism. *Mov Disord* **34**, 1130–1143 (2019).

193. Wilcox, M. V. *et al.* Repeated binge-like ethanol drinking alters ethanol drinking patterns and depresses striatal GABAergic transmission. *Neuropsychopharmacology* **39**, 579–594 (2014).

194. Wyllie, D. J., Béhé, P. & Colquhoun, D. Single-channel activations and concentration jumps: comparison of recombinant NR1a/NR2A and NR1a/NR2D NMDA receptors. *J Physiol* **510 (Pt 1)**, 1–18 (1998).

195. Xiao, X. *et al.* A Genetically Defined Compartmentalized Striatal Direct Pathway for Negative Reinforcement. *Cell* **183**, 211-227.e20 (2020).

196. Yasukawa, T., Kita, T., Xue, Y. & Kita, H. Rat intralaminar thalamic nuclei projections to the globus pallidus: a biotinylated dextran amine anterograde tracing study. *J Comp Neurol* **471**, 153–167 (2004).

197. Yin, H. H. & Knowlton, B. J. The role of the basal ganglia in habit formation. *Nat Rev Neurosci* **7**, 464–476 (2006).

198. Zhang, X., Feng, Z.-J. & Chergui, K. Allosteric modulation of GluN2C/GluN2D-containing NMDA receptors bidirectionally modulates dopamine release: implication for Parkinson's disease. *Br J Pharmacol* **171**, 3938–3945 (2014).

199. Zhang, X. & Chergui, K. Dopamine depletion of the striatum causes a cell-type specific reorganization of GluN2B- and GluN2D-containing NMDA receptors. *Neuropharmacology* **92**, 108–115 (2015).

200. Zhang, X., Feng, Z.-J. & Chergui, K. GluN2D-containing NMDA receptors inhibit neurotransmission in the mouse striatum through a cholinergic mechanism: implication for Parkinson's disease. *J Neurochem* **129**, 581–590 (2014).